X-525-64-203

TM X-55084

APPLICATION OF EDDY CURRENT CLUTCHES TO TRACKING ANTENNA DRIVE SYSTEMS

BY
NICHOLAS A. RAUMANN

JULY 1964

NASA
GODDARD SPACE FLIGHT CENTER
GREENBELT, MARYLAND

TABLE OF CONTENTS

LIST OF ILLUSTRATIONS

LIST OF ILLUSTRATIONS (continued)

APPLICATION OF EDDY CURRENT CLUTCHES TO TRACKING ANTENNA DRIVE SYSTEMS

by

Nicholas A. Raumann
Goddard Space Flight Center

1. INTRODUCTION

Large microwave tracking antennas often require servo drive systems capable of delivering several hundred horsepower to control the position of the reflector. This is particularly true for antennas that are not equipped with radomes and are required to operate in strong winds. Antenna specifications usually put severe constraints on the characteristics of the servo system. The drive system must have a large dynamic range. It sometimes must be capable of tracking the trajectory of a missile being fired at close range on one hand, and must also be capable of tracking a synchronous satellite on the other. Tracking has to be accomplished with a minimum of error, typically a minute of arc, but in extreme cases the error has to be less than a few seconds of arc. During the tracking operation the servo system has to show reasonable stability and must be relatively insensitive to environmental conditions such as ice, snow, rain, wind, and heat. The drive system must not generate radio frequency interference (RFI) inasmuch as this would interfere with signals received.

Probably 95% or more of all tracking antennas in operation today make use of dc motor or hydraulic servo drive systems. This is due to the fact that these systems display most of the desirable characteristics and are also most familiar to system designers. But there are other types of drive systems which may perform as well or exceed the performance of the two popular approaches. The eddy current clutch drive is one. Among others are ac variable frequency drives (Lear Siegler) and "Motron" torque converter drives (W. C. Robinette Co.).

The intent of this report is to study the feasibility of an eddy current clutch drive application to an 85 ft antenna system of the type installed in Fairbanks, Alaska, and Rosman, North Carolina.

2. CONSTRUCTION AND CHARACTERISTICS OF EDDY CURRENT CLUTCH

Before discussing an eddy current clutch drive system, it may be of interest to discuss the clutch as a component. The clutch can be thought of as an ac squirrel-cage motor which has been modified to permit independent motion of the rotor and stator with respect to each other and with respect to the frame. A dc winding sets up a magnetic field which induces squirrel-cage currents in the rotor when there is relative motion of the rotor with respect to the stator or drum. To obtain relative motion, the drum is driven by a constant speed motor. If the output shaft connected to the rotor is at a different speed, a torque is developed proportional to the flux of the dc field. For discussion purposes a clutch which has been suggested for the drive system of an 85 ft antenna will be used.

2.1 Construction and Magnetic Circuit

Fig. 1 shows a cutaway view of a standard 220 hp eddy current clutch. Basically the coupling consists of three parts: the driven input

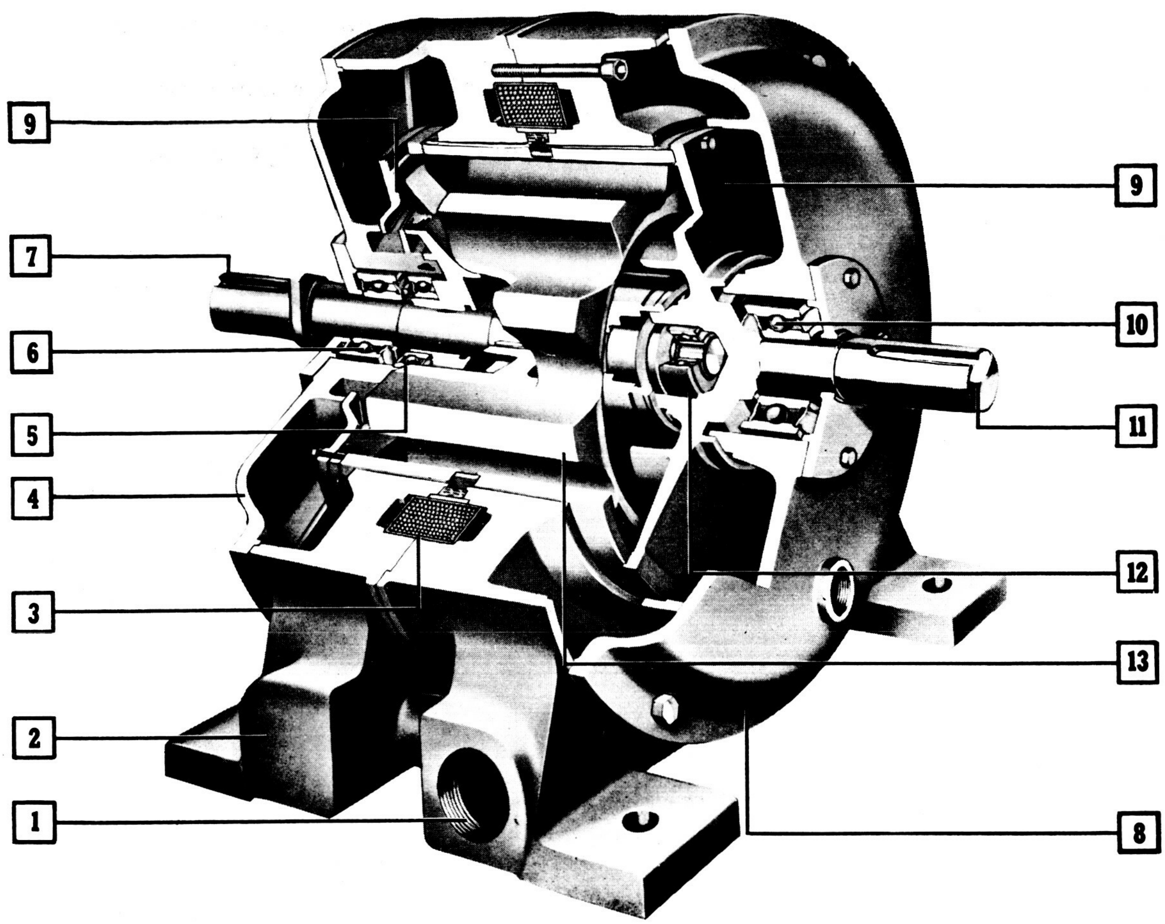

stationary parts

1 water discharge

2 cast frame

3 coil

4 output end bell

8 input end bell

input assembly

Drum [9] and input shaft [11] assembly is carried on two greasable anti-friction bearings, one in input end bracket [10] and other in output end bracket [5].

output assembly

Rotor [13] is mounted on output shaft [7] which is carried on one greasable anti-friction bearing in output end bracket [6] and one pre-lubricated anti-friction pilot bearing [12].

Figure 1—220 hp Eddy Current Clutch (Eaton Manufacturing Co. WCS 216) or drum assembly, the driving output or rotor assembly, and the stationary field assembly. The drum assembly, which is made up of the drum and the input shaft, is supported on two greasable anti-friction bearings, one in the input and the other in the output end bells. In operation, this assembly is the constant speed member driven by a prime mover such as an induction or synchronous motor. The drum is mounted concentrically between the rotor and field assemblies. The rotor assembly consisting of rotor and output shaft is similarly supported by two greasable anti-friction bearings in the input and output end bells. The output shaft is usually connected to the load. In this particular design, the rotor is shaped such that twelve pole sections are established with twelve non-magnetic areas between poles. The field assembly consists of an enclosed toroidal coil and is embedded in the frame of the clutch. A magnetic barrier is placed alongside the coil to prevent a magnetic circuit closure entirely in the field assembly. The advantage of a stationary field is lack of sliprings or commutators which have wear problems and are also a source of RFI.

When the field is excited with dc current, lines of magnetizing force or lines of magnetic intensity are set up as shown in Fig. 2. The lines, after leaving one side of the field assembly, pass through one side of the drum assembly to the poles of the rotor and then return through the other side of the drum back to the field assembly. Both sides of the field and drum assemblies are separated by magnetic barriers. Fig. 3 shows the flux distribution in the clutch. There is a flux concentration in the vicinity of the poles because the flux lines follow a path of minimum reluctance.

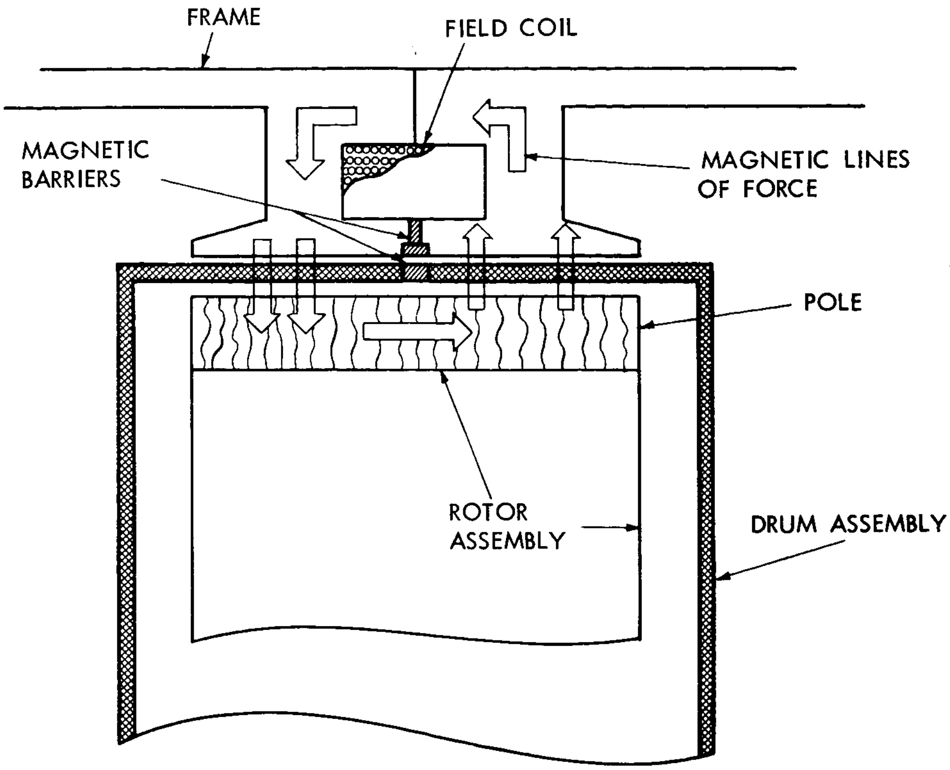

Figure 2—Lines of Magnetic Intensity

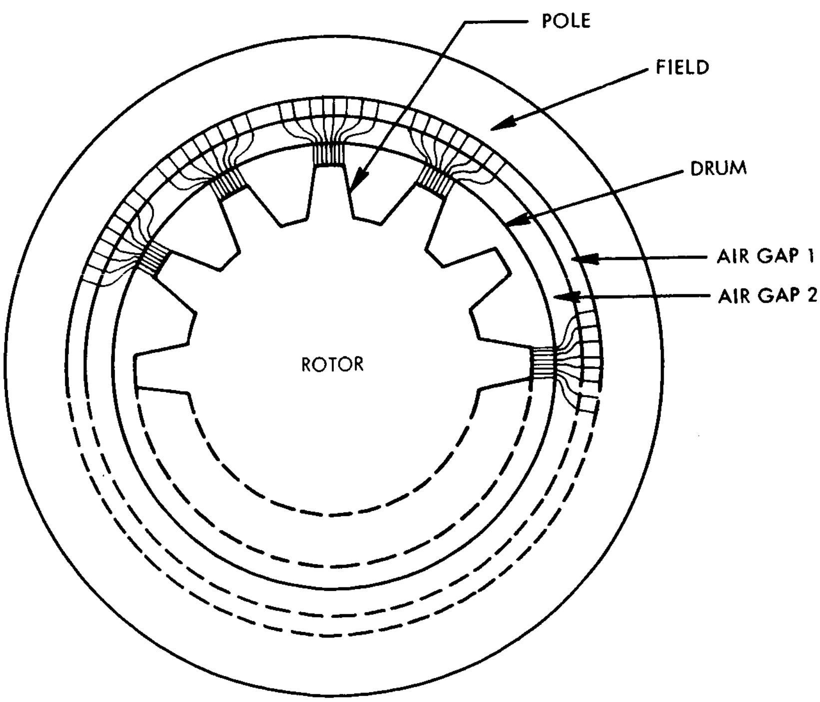

Figure 3—Flux Distribution in Clutch

If relative motion exists between drum and rotor, it can be seen that the flux at any point in the drum changes continuously and thus produces eddy currents in the drum. These currents set up a field which interacts with the field set up by the coil to produce torque.

The interior of the clutch is sealed to permit liquid cooling. Use is made of the constant speed input shaft to circulate the coolant to all critical parts. Normally the coolant is water, but other liquids can be used to accommodate low temperatures.

2.2 Characteristics

The eddy current clutch is a device that can develop torque only in one direction; therefore two clutches are required in systems where load reversal is required. But this consideration is not a disadvantage as far as antenna systems are concerned because opposite or push-pull drives minimize backlash in the gear trains. Push-pull operation also tends to linearize the transfer characteristics of the clutches. Fig. 4 shows the speed-torque curves of a typical clutch. The shape of the curves is very similar to that of ac squirrel-cage motors (NEMA type C or type D operation). Above slip speeds of 600 rpm the curves are virtually flat indicating a lack of damping. Since this is the primary region of operation for antenna application, the eddy current clutch can be considered to be a double integrating device. Dc motors, because of back emf, and hydraulic motors, because of back pressure, can be considered to be single integrators. This makes dc and hydraulic motors velocity controllers, whereas clutches would be acceleration controllers.

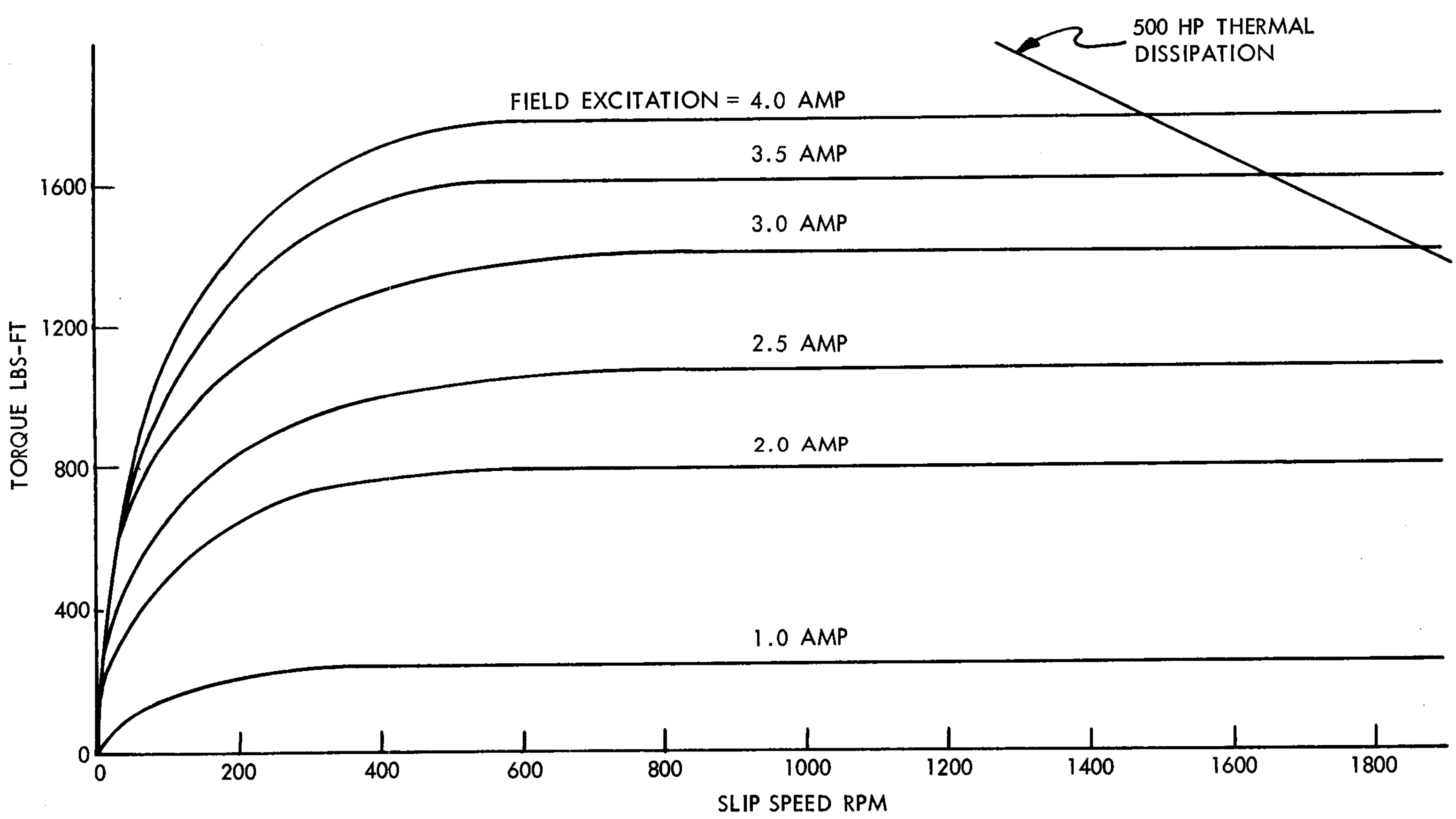

Figure 4—Speed-Torque Characteristic

The speed-torque curves (Fig. 4) can be transposed into a current-torque curve (Fig. 5). This curve shows an approximation to a square-law characteristic for the individual clutch, but shows a linear characteristic (over a large band) for the push-pull combination of clutches. The square-law characteristic is exhibited because both dc flux and induced eddy currents increase with an increase in control current. The push-pull linearization effect can also be shown analytically; if

T = torque – ft lbs

I = current in eddy current clutch field – amps

I_0 = bias current in eddy current clutch field – amps (for Fig. 5, I_0 corresponds to the current that produces 20% rated torque)

K_t' = torque constant – ft lbs/amp/amp bias

then clutches 1 and 2 develop torques:

$$T_1 = K_t' (I_0 + I)^2 \tag{1}$$

$$T_2 = K_t' (I_0 - I)^2 \tag{2}$$

and push-pull operation will yield the combined torque T:

$$T = T_1 - T_2 = 4K_t' I_0 I = K_t \, I \tag{3}$$

The combined torque T, therefore, is a linear function of field current I for constant torque constant K_t' and bias current I_0.

Since two fields are set up in the eddy current clutch, two distinct time constants could be expected: a field time constant, and an eddy current time constant. The inertial time constant prominent in dc and

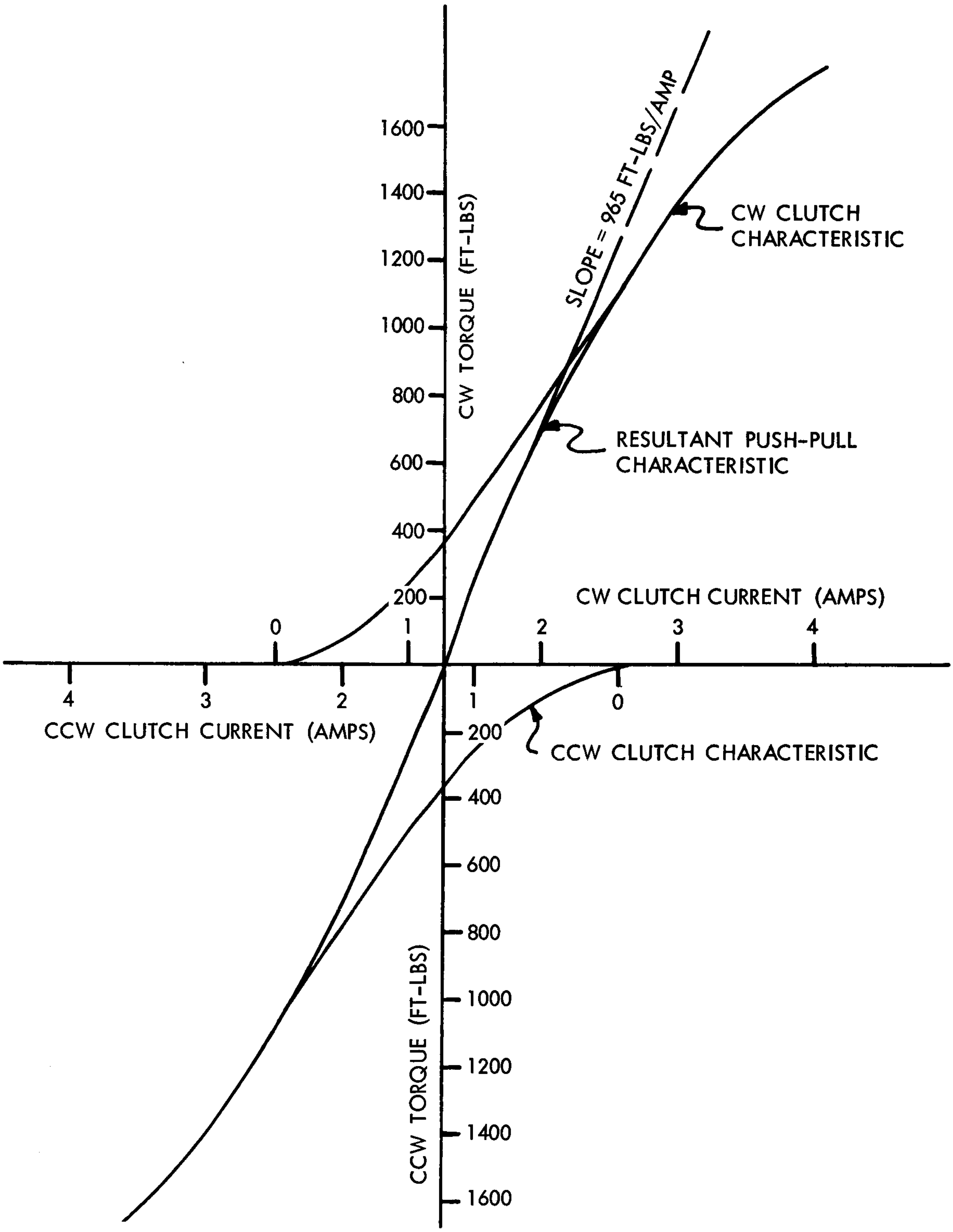

Figure 5—Locked-Rotor Current-Torque Characteristic

hydraulic motors is absent. Test results on clutches indicate that the eddy current time constant is very small and that the field time constant is not a simple time constant in the sense of representing a corner frequency on the Bode plot. Analytical determination of the field time constant is very difficult because clutch geometry enters into the calculation and requires the solution of complicated field problems. However, if simplifying assumptions are made, i.e., assuming simple geometry and ignoring leakage currents and ampere-turns required to set up flux in the steel, the time constant can be computed as follows:

The inductance L of the field can be determined from

$$L = \frac{N\phi}{I} \quad \text{henries} \tag{4}$$

where

N = number of field turns

ϕ = flux - webers

I = field current - amps

The flux ϕ can be determined by

$$\phi = \frac{F}{R} \quad \text{webers} \tag{5}$$

where

F = $4\pi NI$ = magnetomotive force (mmf) - pragilberts

R = total reluctance - pragilberts/weber

The total reluctance R of a simple series magnetic circuit is simply the sum of the reluctance of the steel R_s and the reluctance of the airgap R_a.

Assuming that leakage flux can be neglected, the flux in the steel ϕ_s has to equal the flux in the airgap ϕ_a or

$$\phi_s = \phi_a \tag{6}$$

But since the flux in the airgap is

$$\phi_a = \frac{F}{R_a} \tag{7}$$

equations 5, 6, and 7 can be combined to yield

$$\phi = \frac{4\pi NI}{R_a} \tag{8}$$

The reluctance of the airgap R_a is

$$R_a = \frac{\ell_a}{\mu_a A_a} \text{ pragilberts/weber} \tag{9}$$

where

ℓ_a = length of the airgap – meters

μ_a = permeability of the air = 10^{-7} weber/pragilbert – meters

A_a = area of the pole surface – meters^2

Combining equations 4, 8, and 9:

$$L = \frac{4\pi \mu_a N^2 A_a}{\ell_a} \text{ henries} \tag{10}$$

The resistance of the field coil can be either measured directly or computed by

$$R = 2\pi r \rho N \tag{11}$$

where

r = mean radius of coil - feet

ρ = resistivity of wire - ohms/ft

In using equations 10 and 11 the time constant of the field T_f can be found:

$$T_f = \frac{L}{R} = \frac{2\mu_a NA_a}{\ell_a r\rho} \text{ sec} \tag{12}$$

For more detailed analysis of the transient behavior of clutches the reader is referred to reference 2. With the L and the R of the field coil found the transfer function can be determined for a simple inertial load. The system has two basic equations (in linear range of operation):

$$E = (sL + R) I \tag{13}$$

$$T = K_t I = s^2 J\theta \tag{14}$$

where

E = applied voltage to field - volts

T = torque at output shaft - ft/lbs

J = sum of motor and load inertia - slug ft^2

θ = output shaft position – radians

s = Laplace operator

Combining equations 12, 13, and 14 gives the transfer function of the eddy current clutch:

$$\frac{\theta}{E} = \frac{K_t/JR}{s^2\,(sT_f + 1)} \tag{15}$$

Another very important characteristic of the coupling is its ability to dissipate heat. Fig. 6 shows the variation of the different power quantities as a function of clutch speed for maximum excitation of the field. The different power quantities can be determined as follows:

$$\text{Input horsepower} = \frac{\text{input speed} \times \text{torque}}{5250} \tag{16}$$

$$\text{Slip horsepower} = \frac{\text{slip speed} \times \text{torque}}{5250} \tag{17}$$

$$\text{Output horsepower} = \frac{\text{output speed} \times \text{torque}}{5250} \tag{18}$$

where: torque = input torque = output torque

slip speed - input speed - output speed

The above expressions are not exact, inasmuch as certain losses have been neglected. These additional losses break down as follows:

Coolant drag loss	= 5%
–with overhauling load	= 10%
Magnetic drag	= 1%

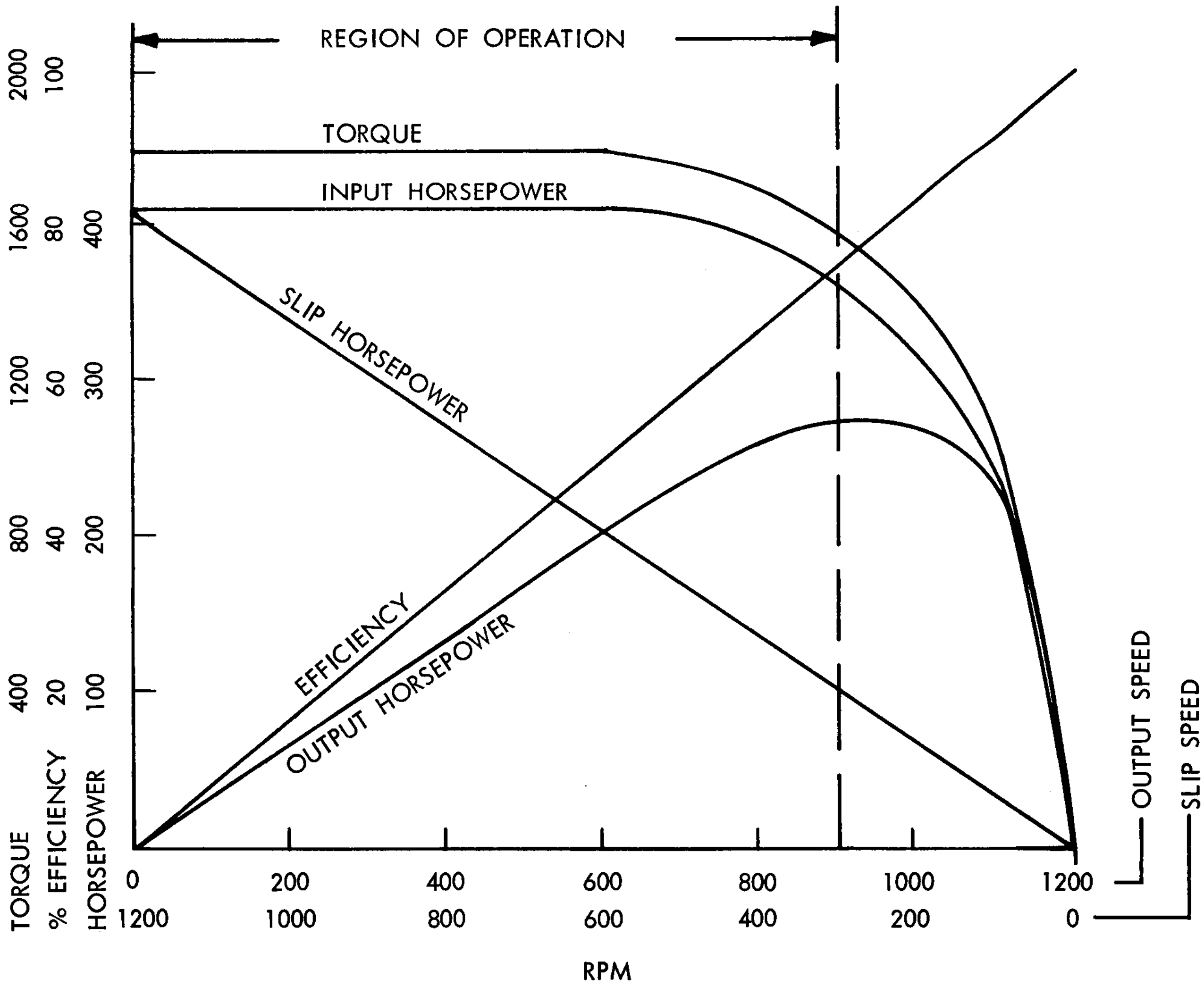

Figure 6—Horse Power Performance Characteristic

Coolant acceleration loss	= .75%
Windage and friction	= .75%
Field excitation loss	= .06%
–with 5:1 forcing	= .4%

It can be seen from Fig. 6 that the heat generated in the clutch is appreciable, especially at low speeds, and care has to be taken that sufficient coolant is supplied to remove the heat from the critical portions of the clutch. This also implies that, if a pair of opposing clutches is at standstill with no load torques applied and a 20% bias is used, $2 \times 0.20 \times 410 = 164$ hp is generated in heat continuously. This is a fair amount of heat to be removed by the coolant and warrants careful economic and reliability type considerations. This heating condition in the clutch represents a major disadvantage of an eddy current clutch system.

The efficiency of the clutch is determined by:

$$\text{Efficiency} = 100 \, \frac{\text{output horsepower}}{\text{input horsepower}} = 100 \, \frac{\text{output speed}}{\text{input speed}} \tag{19}$$

Consequently, low efficiencies are experienced at low clutch output speeds, a condition most commonly occurring in antenna applications.

3. EDDY CURRENT CLUTCH SIMULATOR

Because the eddy current clutch drive system is a rather unfamiliar device, a scaled-down simulator was built rather than a full-size drive for an 85 ft acquisition antenna. The simulator allows the evaluation of system and component characteristics in the laboratory and shows trends and design requirements for the full-size version. The simulator was built for NASA by Westinghouse Electric Corporation under contract NAS5-2916 (see reference, 1). The simulator is shown in Figs. 7 and 8. Basically, the simulator consists of a pair of eddy current clutches with drive motors, a gear box, a load, a controller, and a pair of power amplifiers. When torque requirements were scaled down by a factor of 2000 and speeds were scaled up by 65, a reasonably sized simulator was obtained. Table 1 lists important characteristics of an 85 ft antenna and its corresponding simulator quantities.

Table 1 – System Characteristics

Quantity	Symbol	Units	85 ft Antenna	Simulator
Load inertia	J_L	slug ft^2	7.1×10^6	55
Wind torque	T_W	ft lbs	1.0×10^6	496
Load velocity	$\dot{\theta}_L$	rpm	.5	33.5
Load acceleration	$\ddot{\theta}_L$	rad/sec^2	.0872	5.66
Accuracy		min	.5	32.5
Bandwidth		cps	.7 - 1	.7 - 1
Nat. frequency (antenna reflector)	f_n	cps	1.5	1.67
Nat. frequency (antenna tower)		cps	5.0	5.55

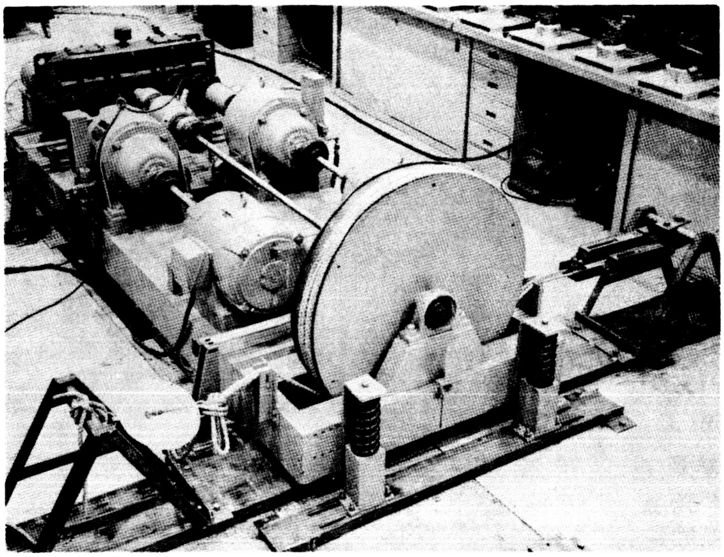

Figure 7–Eddy Current Clutch Simulator (Flywheel End)

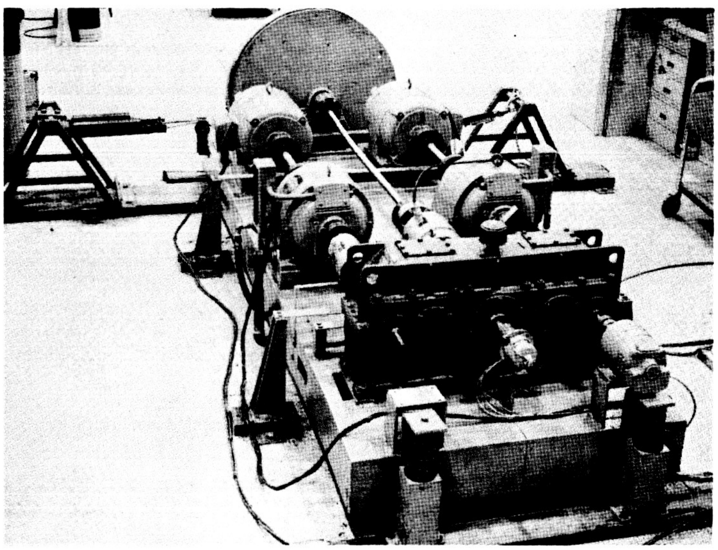

Figure 8–Eddy Current Clutch Simulator (Gearbox End)

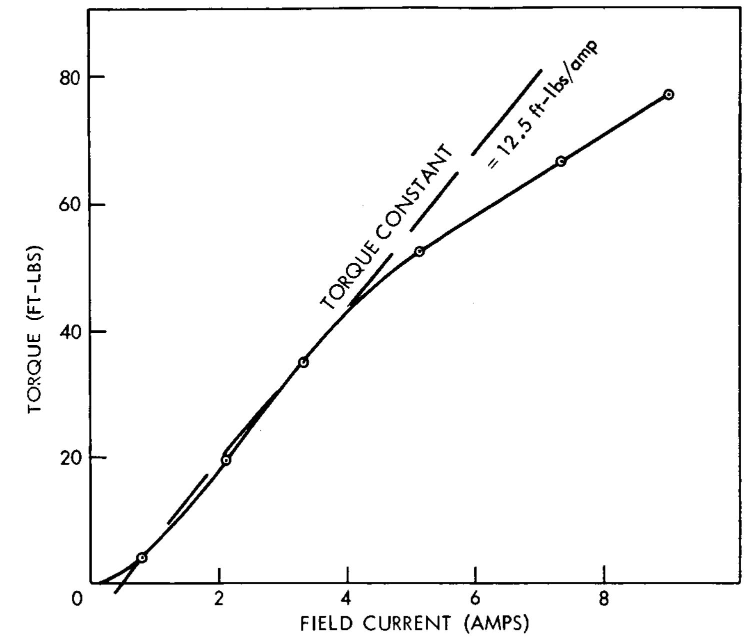

Figure 9—Locked-Rotor Current-Torque Characteristic (Simulator)

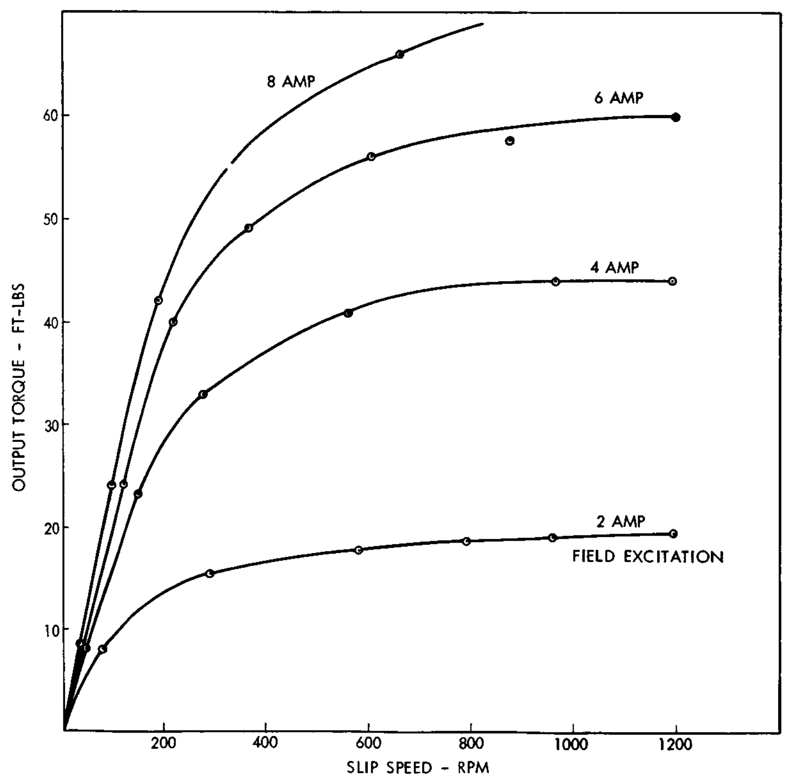

Figure 10—Speed-Torque Characteristic (Simulator)

3.1 Simulator Clutches

WCS 2062 clutches were selected for the simulator. These are standard 10 hp watercooled units and are driven by 10 hp, 1160 rpm squirrel-cage motors. The clutches are manufactured by Eaton Manufacturing Company. To study the performance of these clutches, a series of characteristic curves were obtained.

Current – Torque Characteristic (Fig. 9): The curve shows how torque varies with field current under locked-rotor conditions. For low excitations the square-law characteristic is exhibited and at high excitations the effect of saturation becomes noticeable. The straight line portion of the curve has a slope of 12.5 ft lbs/amp.

Speed – Torque Characteristic (Fig. 10): The curve shows variation of torque with respect to speed for various excitation conditions. Especially of interest is the slope of the curves because the slope is a measure of the inherent damping of the clutch. For a given excitation very little damping is obtained at high slip speeds, and high damping is obtained at low slip speeds. Thus the amount of damping is a function of speed. But, if operation is confined to the high slip speed end of the curve–say between 600 and 1200 rpm, virtually constant damping is encountered. If different excitation levels are now considered, a dependency between damping and excitation level is found with damping being proportional to excitation.

Torque – Time Response (Fig. 11): Fig. 11a shows the current and torque response to an increasing step in voltage. The current jumps to about 21% of its final value and then continues to rise exponentially with

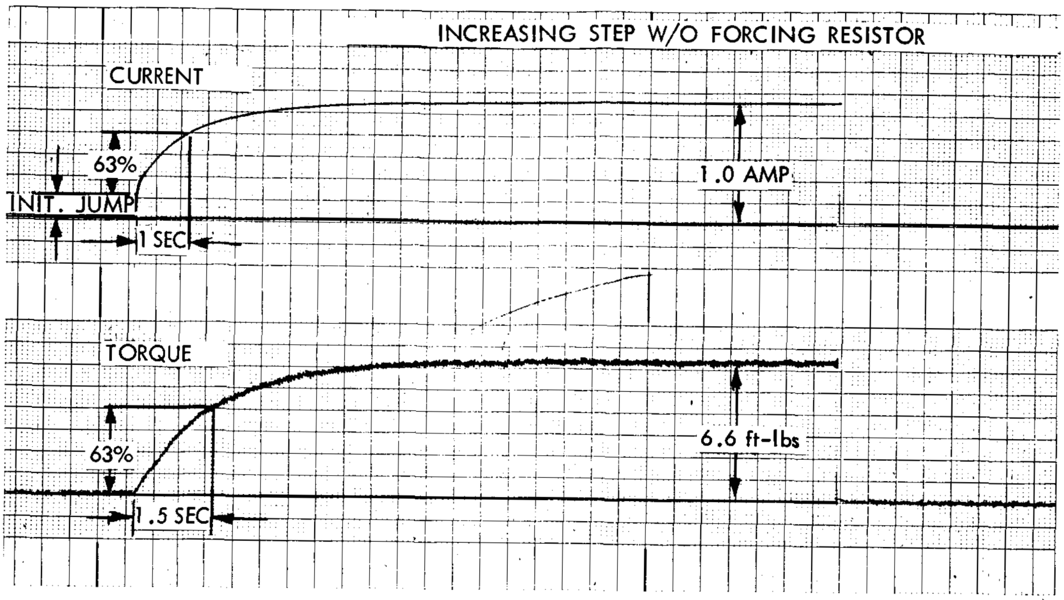

Figure 11a—Transient Response-Increasing Step w/o Forcing Resistor

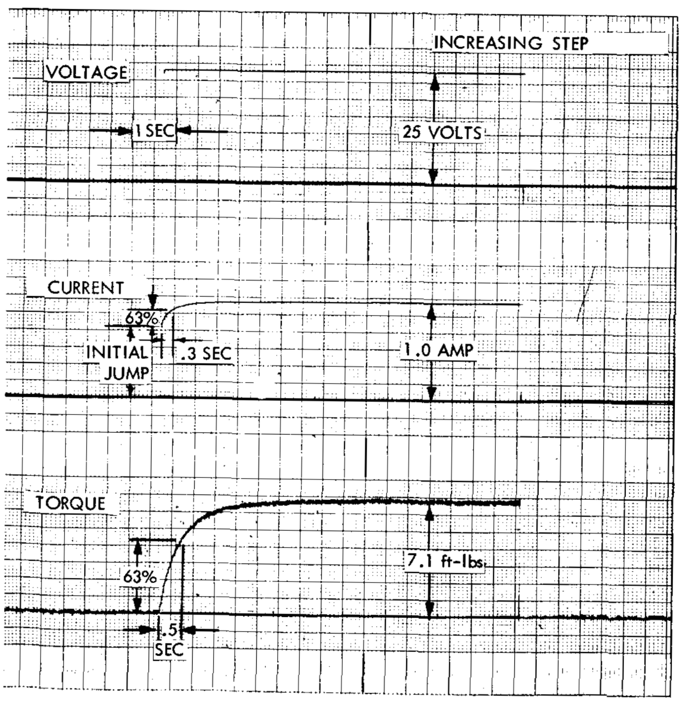

Figure 11b—Transient Response-Increasing Step

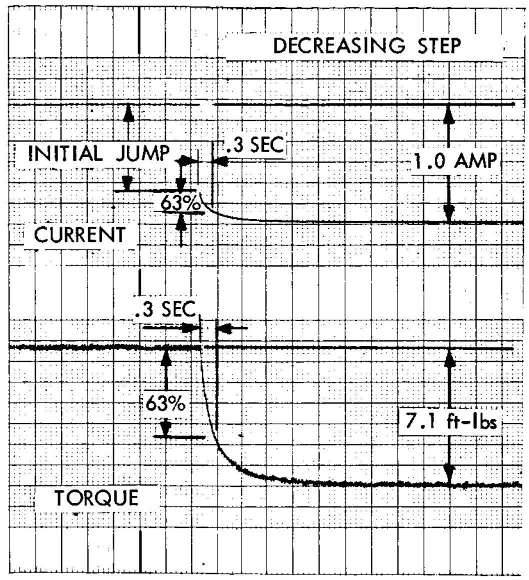

Figure 11c—Transient Response-Decreasing Step

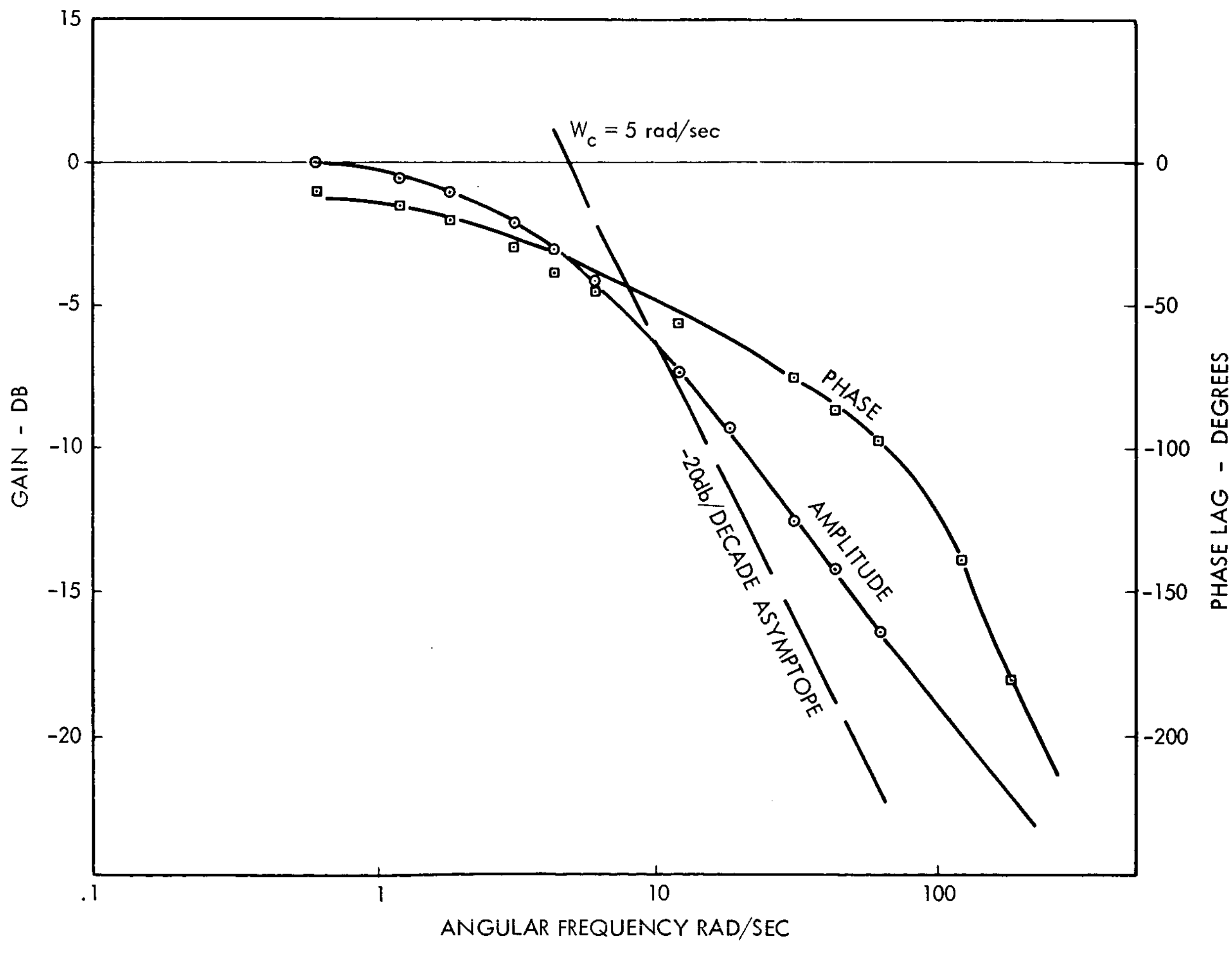

Figure 12—Frequency Response of Clutch

an approximate time constant (63% of final value) of 1.0 sec. The torque does not have an initial jump but rises exponentially with a time constant of 1.5 sec. The linear relationship between torque and current observed in ac and dc machines therefore seems to be missing in eddy current clutches. To reduce the torque time constant, an external forcing resistor can be used. In the case of the simulator 10:1 forcing was utilized; i.e., in series with the 2.3 ohm field of the clutch a resistor of 23 ohms was added. The time response for this condition is shown in Fig. 11b. Now the current jumps to 75% of its final value and continues to rise with a time constant of 0.3 sec. The torque response displays a time constant of 0.5 sec. Consequently, field forcing of 10:1 has improved the torque time constant by 3:1 only. Fig. 11c shows the response for a decreasing step in voltage. The current characteristic is very similar to that of the preceding case, but the torque decays faster with a time constant of 0.3 sec. Other tests performed indicated that the time constant does not seem to be affected much by the size of the voltage step applied, and also not by the amount of bias current used.

Torque – Frequency Response (Fig. 12); The frequency response shows approximately the characteristics of a single time constant device with a corner frequency at 5 rad/sec (time constant = .2 sec); however, closer investigation reveals that a rather poor correlation between the amplitude response and the -20 db/decade asymptote is obtained. The corresponding phase shift is larger than that of a single time constant device and shows marked similarity to a non-minimum phase network.

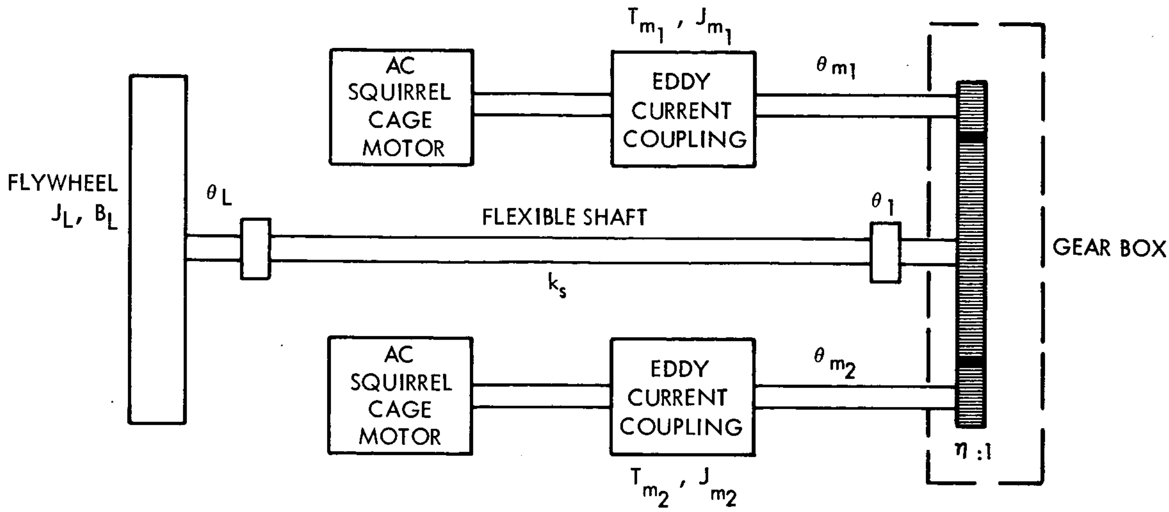

Figure 13a—Block Diagram of Mechanical Arrangement of Simulator

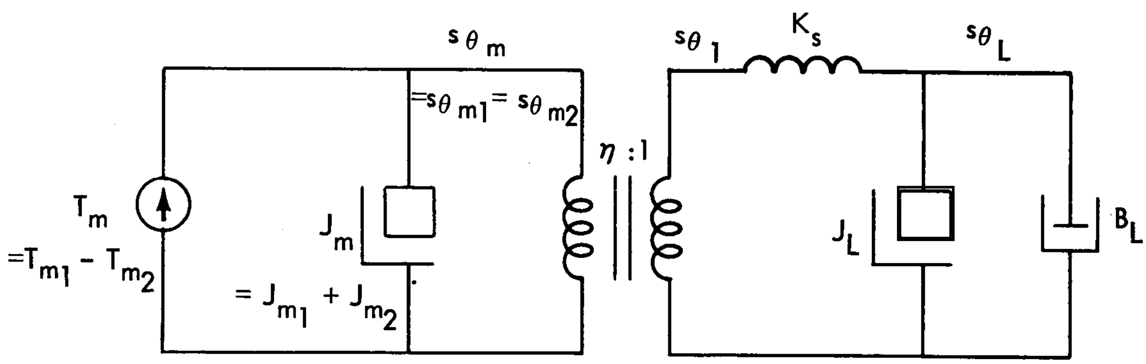

J_{m_1}, J_{m_2} = eddy current clutch inertia (including equivalent inertias of gear train, pinions, couplings, etc.)

T_{m_1}, T_{m_2} = output torque of clutch

θ_{m_1}, θ_{m_2} = shaft position of clutch

μ = gear ratio

θ_1 = position of output shaft of gear box

K_s = spring constant of shaft

J_L = load inertia

B_L = load friction

θ_L = shaft position of load

S = Laplace operator

Figure 13b—Equivalent Mechanical Circuit

Based on these and preceding observations it can be concluded that the eddy current clutch has several inherent non-linearities which would rule out linear system analysis like Bode plot design, Root locus method, etc. However, for a first approximation in system design a linearized clutch transfer function of the form given in equation 15 could be used. It is difficult to say whether the non-linearities observed in the clutch tested will become worse in larger sized units and, if so, to what degree.

3.2 Mechanical Load

The load of the simulator consists of a flywheel which represents the scaled down inertia of the reflector of an antenna and a flexible shaft which, together with the flywheel, simulates the natural frequency of the reflector. A block diagram and a simplified equivalent circuit of the mechanical system are shown in Fig. 13. From the equivalent circuit two basic equations can be written:

$$nT = s^2 n J_m \theta_m + K_s \left(\frac{\theta_m}{n} - \theta_L\right) \qquad (20)$$

$$0 = K_s \left(\theta_L - \frac{\theta_m}{n}\right) + (s^2 J_L + s B_L)\, \theta_L \qquad (21)$$

Solving these equations simultaneously gives the transfer function of the mechanical system:

$$\frac{\theta_L}{T} = \frac{n/B_L}{s\left[\frac{n^2}{K_s B_L} J_m J_L s^3 + \frac{n^2 J_m}{K_s} s^2 + (n^2 J_m + J_L) \frac{1}{B_L} s + 1\right]} \tag{22}$$

Since the friction in the system is small, the assumption can be made that the friction term B_L approaches zero, which simplifies the transfer function to

$$\frac{\theta_L}{T} = \frac{\frac{n}{n^2 J_m + J_L}}{s^2\left(\frac{n^2 J_m J_L}{K_s(n^2 J_m + J_L)} s^2 + 1\right)} = \frac{K_t}{s^2\left(\frac{s^2}{\omega_n^2} + 1\right)} \tag{23}$$

where

$$k_t = \text{torque constant} = \frac{n}{n^2 J_m + J_L}$$

$$\omega_n = \text{natural frequency} = \sqrt{\frac{K_s\,(n^2 J_m + J_L)}{n^2 J_m J_L}}$$

Substituting values for the system constants: J_m = .329 slug ft^2, J_L = 55 slug ft^2, K_s = 5060 ft lbs/rad, and n = 20, then

$$k_t = .107 \text{ rad/ft lbs}$$

$$\omega_n = 11.4 \text{ rad/sec} = 1.82 \text{ cps}$$

$$\frac{\theta_L}{T_m} = \frac{.107}{s^2(.0077\, s^2 + 1)} \tag{24}$$

Fig. 14a shows the response of the mechanical system to an initial torque input. The natural damped frequency is 1.67 cps, therefore correlating with the value computed above. The response has an exponential

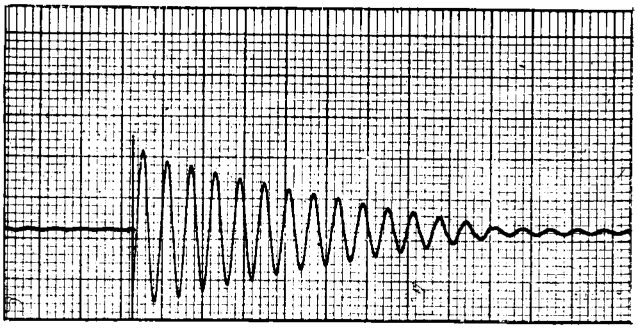

Figure 14a—Natural Frequency of Simulated Reflector

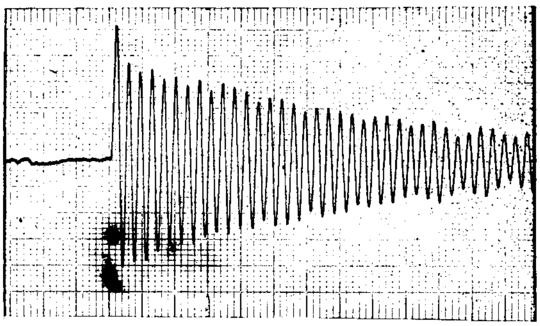

Figure 14b—Natural Frequency of Simulated Antenna Tower

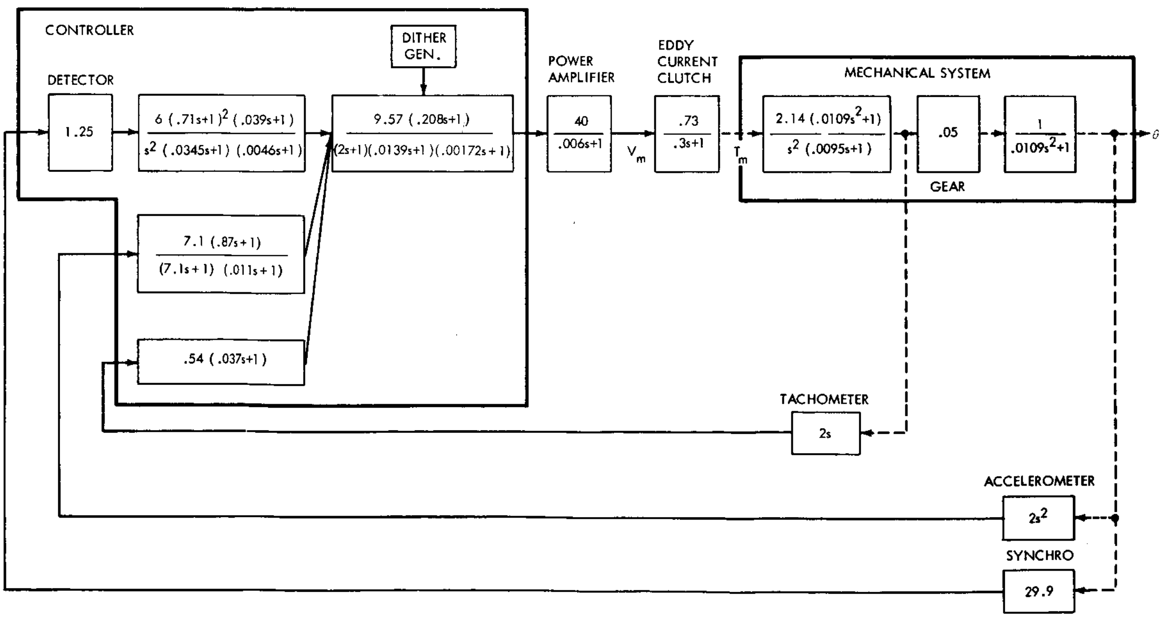

Figure 15—Block Diagram of Control Loop

decay that corresponds to a damping factor of 0.022. This makes valid the previous assumption that the friction term B_L can be neglected.

To simulate the natural frequency of the tower, mechanical components have been mounted on a spring supported bedplate. The bedplate mass-spring combination gives rise to the natural frequency of the antenna tower structure. Fig. 14b indicates a natural frequency for the mass-spring combination of 5.55 cps with a damping factor of about .007. By properly instrumenting the simulator, the effects of reflector and tower frequencies are summed into the overall system servo loop.

3.3 Controller and Power Amplifier

The controller for the simulator uses operational amplifiers as its basic building blocks. The transfer functions of these amplifiers can be readily shaped so as to give desired open and closed servo loop characteristics consistent with stability and accuracy requirements. The controller is capable of demodulating the synchro position error signal and of accepting velocity and acceleration feedback signals. The controller superimposes a dither signal on its output which decreases system coulomb friction, and therefore reduces breakaway torque. The output of the controller drives the power amplifiers.

The power amplifiers, one for each clutch, are capable not only of exciting the field of the clutches but also their forcing resistors. The power amplifiers are 300 volt, 3 phase silicon-controlled rectifier (SCR) ac to dc converters. From an operational requirement, SCR's are hardly desirable because they generate radio frequency interference

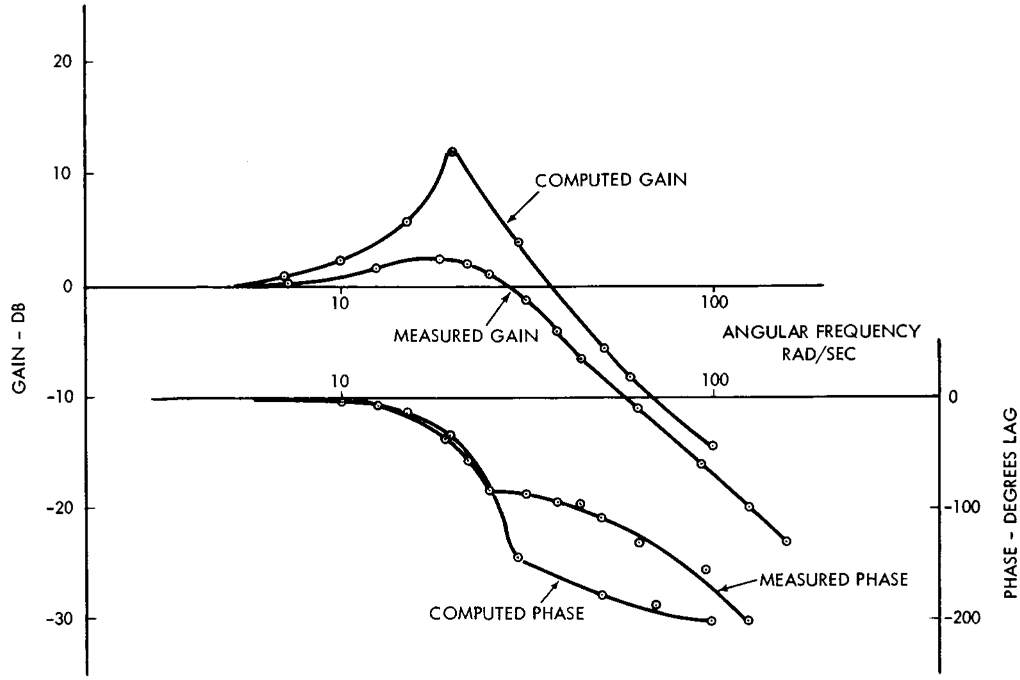

Figure 16a—Bode Plot for Closed Tachometer Loop

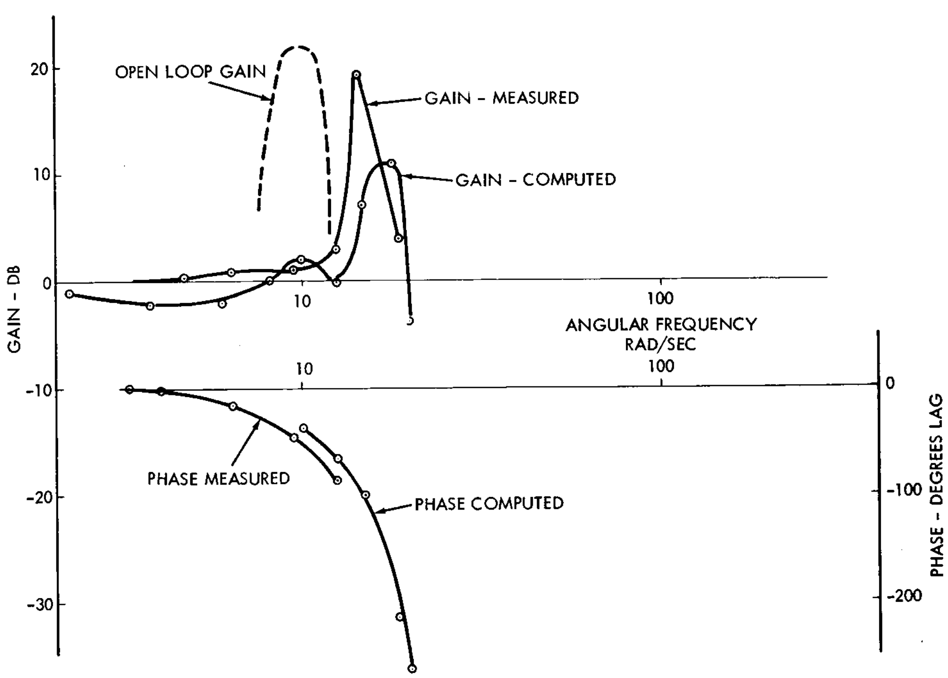

Figure 16b—Bode Plot for Closed Accelerometer Loop

(RFI) due to their steep wave fronts and have an inherent delay (transport lag) which is a considerable fraction of a period of the power supply frequency. Replacement of these amplifiers with "true" dc amplifiers should be considered for similar applications.

3.4 Simulator Performance

From the block diagram of the servo system, as shown in Fig. 15, it should be observed that three distinct loops are used for ultimate system stability and accuracy. Because the eddy current clutch has very little inherent damping, the tachometer loop is used mainly to introduce controllable damping. Fig. 16a shows the closed loop frequency response for this loop and indicates a 3 db bandwidth of 35 rad/sec. The somewhat poor correlation between the measured and computed curves is most likely due to the non-linear behavior of the clutch itself. The primary natural frequency of the load is about 10 rad/sec. Since an overall bandwidth of about 6 rad/sec is required, stability problems are encountered if the position loop were to be closed. The stability problem arises because the natural frequency is very close to the desired cut-off frequency of the position loop and because the load is highly underdamped. It is for this reason that the accelerometer loop is used. As is evident from the Bode plot for this loop (Fig. 16b), the underdamped mode has been shifted out to about 15 rad/sec and damping has been effectively increased.

Open loop gain and bandwidth of the position loop depend on the type of target to be tracked and the allowable tracking accuracy. If one considers a satellite tracking antenna, then the number of classes of possible input functions to the servo system is rather limited to some well-defined continuous functions. For example, functions with discontinuous steps can be ruled out. One can use a simple graphical curve fitting mthod as outlined in reference 5 (pp. 61-65) to obtain equivalent sinusoidal inputs for velocity, acceleration, and higher derivatives. Table 2

Table 2 – Equivalent Sinusoidal Inputs

Quantity	Symbol	Max. Value Given for Antenna (for Simulator X65)	Equivalent	
			Gain -db	Frequency (rad/sec)
Position	θ	$\pm 70^\circ$	88.51	.0256
Velocity	$\dot{\theta}$	$2.8^\circ/\text{sec}$	81.55	.0426
Acceleration	$\ddot{\theta}$	$.1^\circ/\text{sec}^2$	62.68	.154
Jerk	$\dddot{\theta}$	$.014^\circ/\text{sec}^3$	40.20	.307

gives the results of this method for a satellite in a 100-mile circular orbit with an orbital velocity of 4.9 miles/second and a permissible tracking error ϵ of 10 seconds of arc. The choice of the servomechanism type (refer to reference 4, pp. 2-35 to 2-36) to be used in the position loop depends mainly upon the open loop gain required. For the same conditions as above the open loop gains for different type systems are:

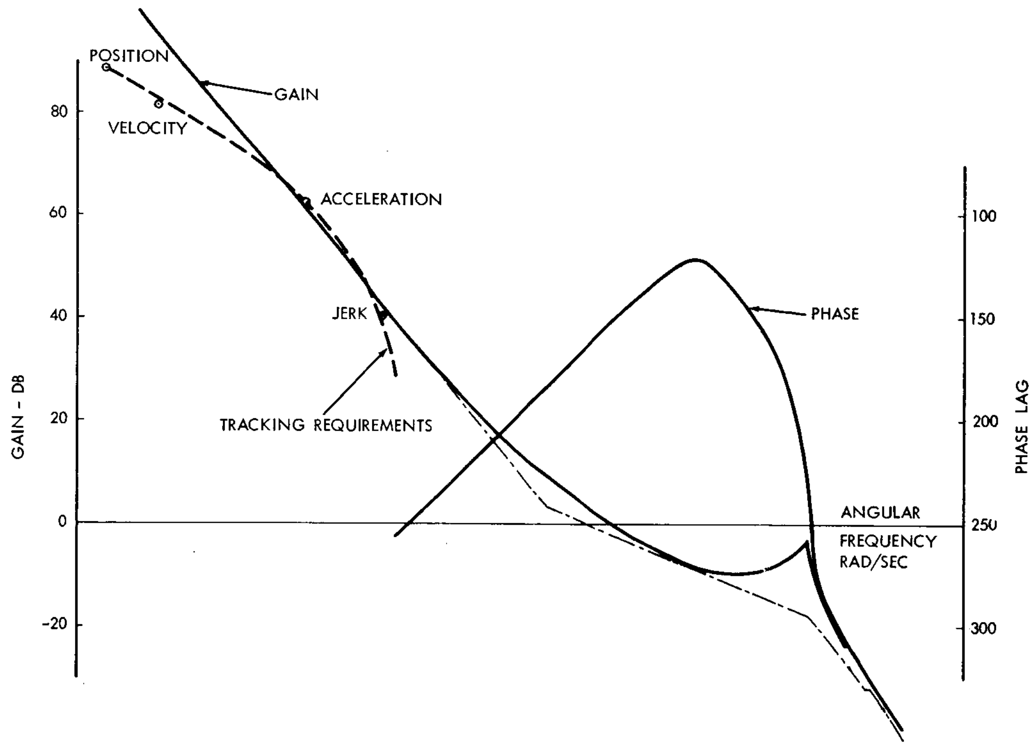

Figure 17a—Bode Plot for Open Position Loop

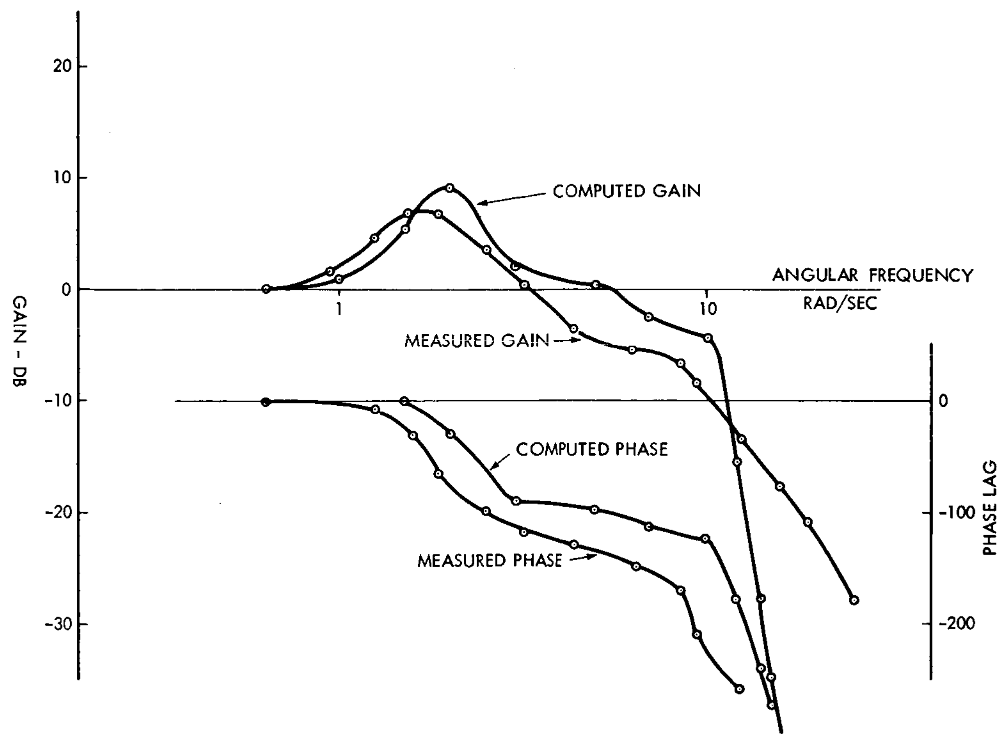

Figure 17b—Bode Plot for Closed Position Loop

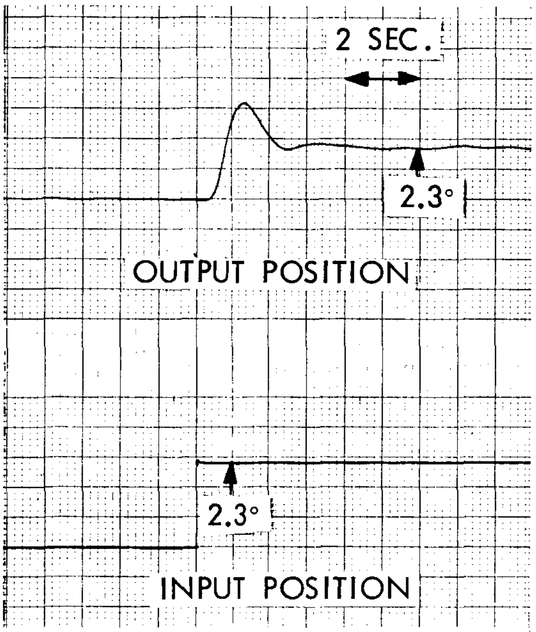

Figure 18a—Step Response of Simulator

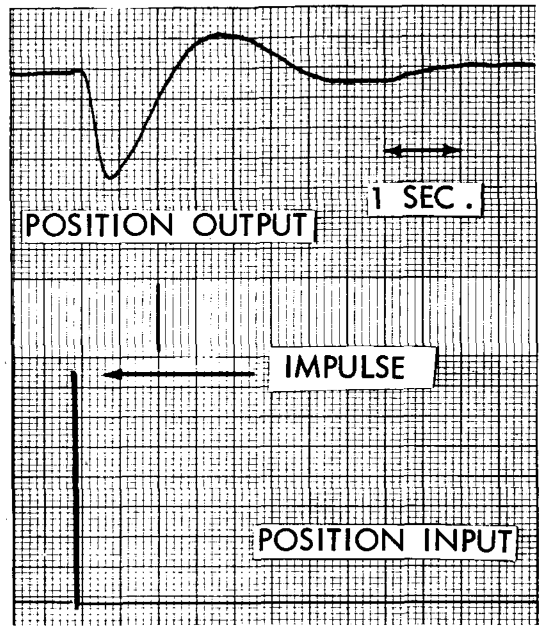

Figure 18b—Impulse Response of Simulator

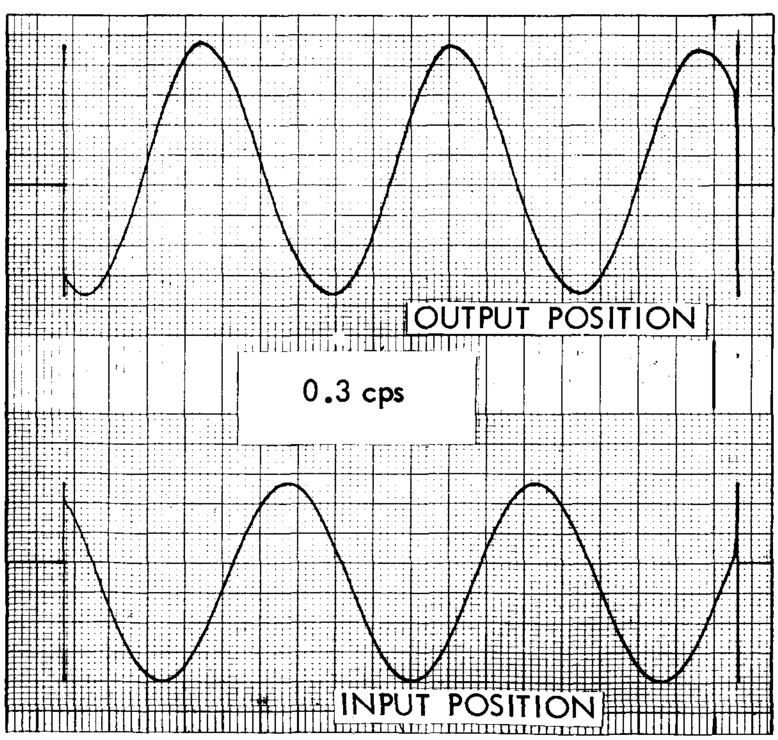

Figure 18c—Sine Wave Response of Simulator

$$\text{Type 1:} \quad K_v = \frac{\dot{\theta}}{\epsilon} = \frac{2.8 \times 3600}{10} = 1010 = 40.1 \text{ db} \tag{25}$$

$$\text{Type 2:} \quad K_a = \frac{\ddot{\theta}}{\epsilon} = \frac{.1 \times 3600}{10} = 36 = 30.5 \text{ db} \tag{26}$$

$$\text{Type 3:} \quad K_j = \frac{\dddot{\theta}}{\epsilon} = \frac{.014 \times 3600}{10} = 5 = 13.9 \text{ db} \tag{27}$$

This high gain type 1 system is undesirable from the standpoint of noise problems, and the lower gain type 3 system has problems in stabilization. Nevertheless, the latter system was chosen because it represented the best compromise. Fig. 17a shows the open and Fig. 17b the closed loop Bode plots for the position loop. The dotted line in Fig. 17a is the graphical representation of results from Table 2. This line defines the open loop gains which have to be realized in order to track with the required accuracy. A closed loop 3 db bandwidth of 4 rad/sec was obtained, which is just below the specification requirements of 4.4 rad/sec, but minor adjustments in the loop could remedy this situation.

Fig. 18a, b, and c show the step, impulse, and sine wave responses, respectively, for the position loop. The step response has a 60% overshoot to a 2.3° step or a peak error of 1.4°. Even though the error exceeds the permissible limit, it is of very little consequence since the step function is an input that would not be experienced normally when tracking a satellite. What is of importance, though, is the fact that after the first overshoot no other overshoots of any sizable amplitude occur, indicating sufficient damping such that oscillations will not be sustained for any large duration. The impulse response, which characterizes the system, shows rapid convergence indicating not only absolute stability, but also the degree of stability.

The response to a sine wave indicates that there is hardly a degradation of the output wave but there is a phase shift consistent with the phase frequency response (Fig. 17b).

A heat run was performed in which the simulator was adjusted so that 9.7 hp was dissipated in one clutch continuously. This is close to the 10 hp maximum thermal capacity of the coupling. During this test, the frame temperature rose 32°F above ambient and the water outlet temperature rose 28°F in about 30 minutes. Computations indicate that about 6 hp of heat was removed by the water coolant while the rest was lost by radiation and conduction to the bedplate and to the surrounding air. The result of this test indicates that there is practically no heating problem and temporary overloads could probably be handled readily.

For other test results particularly covering position errors under different conditions, measurement of coulomb friction and threshold of motion reference 1 should be reviewed.

4. FULL SIZE EDDY CURRENT CLUTCH DRIVE

By using simulator test results and by projecting these to a full-scale version, a full-size eddy current clutch drive can be designed. The drive system could be similar to that proposed by Westinghouse in their report (reference 1) and shown in Fig. 19. The two opposing couplings are mounted on a common bedplate together with their driving motors. The output shafts of the clutches are connected to independent gear paths, which in turn are connected to the sector or bull gear of either

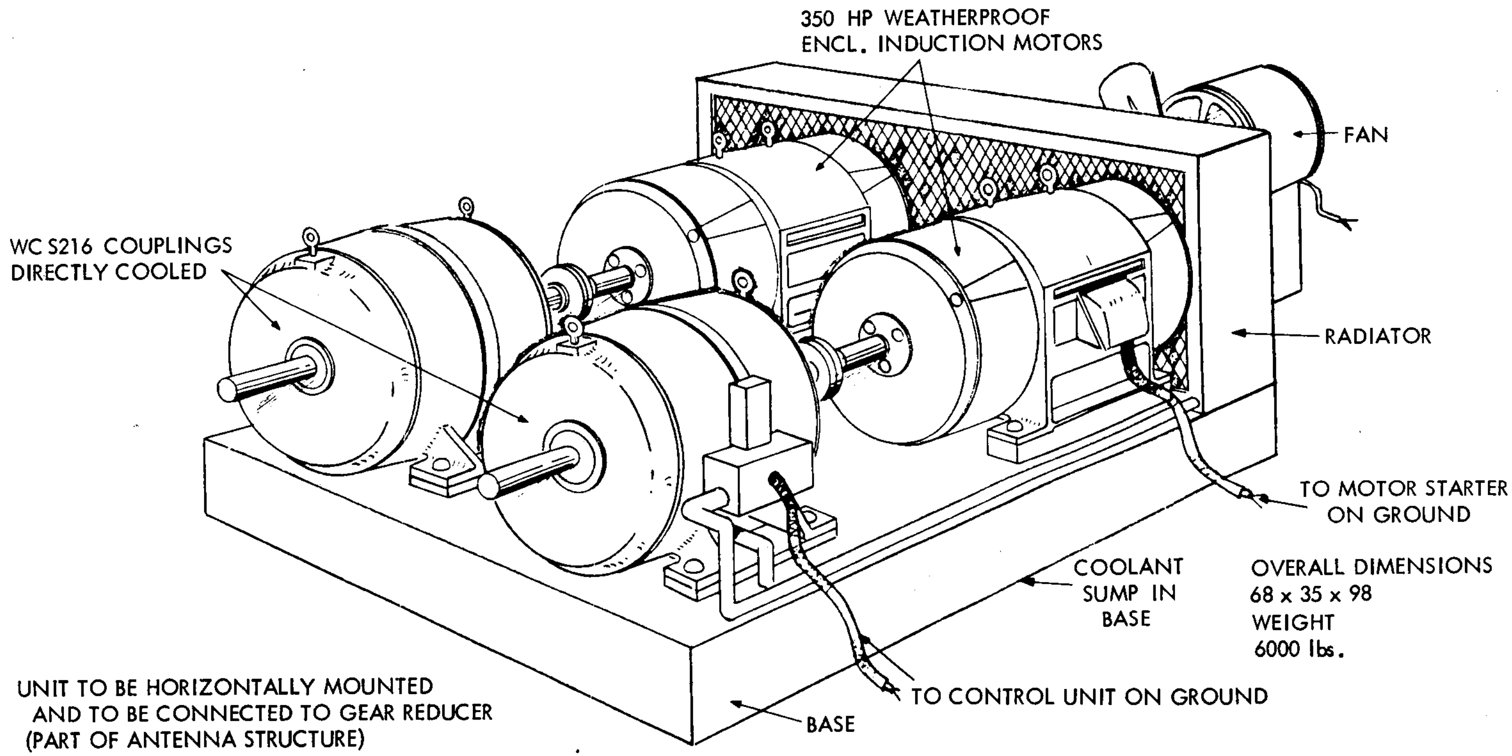

Figure 19—Proposed Layout of Drive System for Full-size Antenna

the X or Y axis of the antenna. The size of the couplings is determined from tracking, slewing, and stowing requirements, taking into account windloading, inertia, and friction effects. It is found that an Eaton WCS 216 clutch can be used on the X-axis and a WCS 215 on the Y-axis. These units can deliver nominally 220 hp and 140 hp respectively. These clutches could be standard production units, but most likely would be modified slightly to improve the field time constant. The driving motors would be standard ac squirrel-cage motors compatible with the horsepower requirement of the clutches. Squirrel-cage motors are chosen because of their efficiency, low cost, and lack of commutators or sliprings.

A closed cycle cooling system consisting of a radiator, a fan, and a sump located directly in the bedplate would be used. A closed cycle system has the advantage of economy and lack of extensive piping and filtering requirements. Normally the coolant for clutches is water, but other coolants can be used. To accommodate temperatures below 32°F, either of two things can be done: heaters can be installed to keep the water temperature above 32°F even in a non-operating condition of the antenna, or glycol can be used as a coolant. Either approach has its advantages and disadvantages, the second approach being favored because power failure will not cause damage to the equipment. However glycol, because of its inherent characteristics, will require twice the flow required of water to remove the same amount of heat. The water demand of the clutch is about 1 gpm for each 10 hp slip or twice that rate when glycol is used. The maximum anticipated flow rate is 30 gpm for glycol. For economy coolant metering will be used, permitting higher flows only when the demand exists. The coolant demand can readily be determined from the discharge temperature of the coolant. This temperature rises as the slip horsepower increases. To prevent flooding of the clutch, free discharge to the sump is essential and is maintained easily for the X-axis drive. For the Y-axis, a problem exists since the bed-plate is not stationary but has freedom to move $\pm 90^\circ$ from horizontal. This causes a problem with free gravitational flow, and flooding could occur since the clutch rotates end-for-end. Use can be made of bevel gears to change the rotation of the clutches from end-for-end to axial, Under this condition, modifications to the outlet ports could yield satisfactory flow if the sump is modified accordingly. The other alternative is to change the coupling from a direct to an indirect cooled unit. In this method coolant reaches the outside of the drum only, reducing cooling efficiency but permitting rotation of the clutch in any direction. This approach is preferred provided the modified thermal horsepower capacity is not exceeded.

Excitation for the fields of the eddy current clutch could be provided from several devices such as dc generators, amplidynes, rototrols, magnetic amplifiers, SCR amplifiers, or transistor amplifiers. Rotating amplifiers have the disadvantage of limited brush and bearing life and are also notorious for RFI generation. SCR amplifiers have the same problem. Eventhough they have no moving parts, they are a source of RFI because of their steep wave fronts. Of course, attempts could be made to filter out RFI by using low-pass filters which do not affect signal frequencies. Filtering will probably be efficient, since the amplifiers are located in the control building rather than on the antenna structure itself. Magnetic amplifiers are very similar in their operation to SCR's, but do not display the steep wave fronts. The disadvantage of magnetic amplifiers is their relatively larger time constant. Ideally suited for this application would be a linear transistor amplifier if it were not for the high power output requirement of over 1 kw. This amount of power is difficult to handle by a linear dc amplifier, although it is not impossible to build one.

The controller for this application would be very similar to that of standard controllers for this type of antennas. The controller could consist of operational amplifiers connected so as to give the desired transfer characteristics. The controller should have a clutch temperature monitor in addition to the ordinary protection devices, such as velocity, position, and torque limits. Because of the high slip horsepowers involved, an automatic temperature monitor should be included which either reduces the power to the antenna drive or shuts it down completely when predetermined limits are exceeded. This precautionary device will prevent costly burnouts of clutches.

It is expected that the dynamic response of the full-size drive will be similar to that of the simulator. Performance of course will be degraded somewhat by factors not taken into account in the simulation. But it is also anticipated that performance will be as good as that of comparable hydraulic drives.

5. COMPARISON

It is difficult to make a flat statement that the eddy current clutch drive is better than the more conventional drives. On the other hand, it is as difficult to say that any other drive is better than the eddy current clutch. Each type of drive has its advantages and disadvantages, and these have to be weighed against each other when considering a particular application. Even then a clear-cut decision is often hard to come by. An attempt will be made here to point out the advantages and disadvantages of some drives and how they compare with the eddy current clutch.

5.1 DC Motor Drive

For high performance dc drives armature-controlled motors are used exclusively. Three types of motors can be considered for control applications: the standard NEMA frame motor, the more specialized servo motor, and the torque motor. Torque motors are low speed, permanent magnet field motors. Their construction is such that they can be mounted on an antenna axis directly without gearing and therefore without backlash that accompanies gearing. Smooth and linear operation can be obtained even at very low speeds. Unfortunately their maximum torque capability is limited to about 10,000 ft lbs on commercially available units, which rules out their application on radomeless 85 ft antennas.

NEMA design motors can be used up to about 200 hp requirements. Above that the inertia of these units becomes the limiting factor. NEMA design motors have a limited dynamic speed range, higher inertia, poorer linearity, larger ripple torque, and higher brake-away torque than their torque motor counterparts. Servomotors are designed to meet control applications better than NEMA design motors do, but are available only up to 10 hp.

All three types of motors can be excited by vacuum tube, solid state, or magnetic amplifiers for the lower hp ranges but almost always require rotating amplifiers for higher hp applications. The most commonly used connection with rotating amplifiers is the Ward-Leonard loop. A simplified schematic is shown in Fig. 20. Often the motors and generators are modified to include series fields for copper loss compensation, interpole fields for reduction of armature reaction, and current feedback to reduce the generator field time constant. The following equations can be written for the Ward-Leonard loop:

$$V_f = (R_f + s\,L_f)\,I_f \tag{28}$$

$$V_g = K_g\,I_f = (R_a + s\,L_a)\,I_a + V_m \tag{29}$$

$$V_m = s\,K_v\,\theta \tag{30}$$

$$T_m = K_t\,J_a = s^2 J\theta \tag{31}$$

These equations can be combined to yield the transfer function of the dc drive:

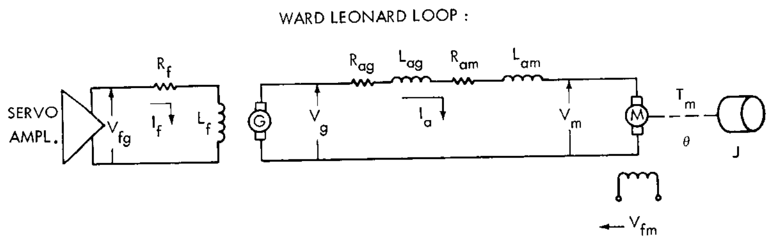

GENERATOR FIELD:

V_{fg} = APPLIED VOLTAGE FROM SERVO AMPLIFIER

I_f = CURRENT

R_f = RESISTANCE

L_f = INDUCTANCE

GENERATOR ARMATURE:

V_g = VOLTAGE

K_g = VOLTAGE CONSTANT

R_{ag} = RESISTANCE

L_{ag} = INDUCTANCE

I_a = CURRENT

MOTOR ARMATURE:

V_m = VOLTAGE

R_{am} = RESISTANCE

L_{am} = INDUCTANCE

K_f = TORQUE CONSTANT

K_v = VOLTAGE CONSTANT

V_{fm} = FIELD VOLTAGE, CONSTANT

LOAD:

J = INERTIA OF LOAD AND MOTOR

T_m = TORQUE

θ_i = LOAD POSITION

$R_a = R_{ag} + R_{am}$

$L_a = L_{ag} + L_{am}$

Figure 20—Electrical Drive System

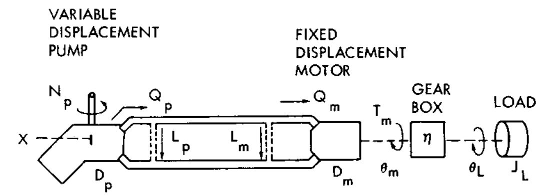

NOTATION:

PUMP

X = TOTAL STROKE

X_v = STROKE TO GIVE VELOCITY TO LOAD

X_a = STROKE TO GIVE ACCELERATION TO LOAD

X_c = STROKE TO SUPPLY COMPRESSIBILITY FLOW

N_p = PUMP SPEED

Q_p = PUMP FLOW

L_p = PUMP LEAKAGE

D_p = DISPLACEMENT OF PUMP

B = BULK MODULUS

V = VOLUME OF OIL UNDER COMPRESSION

K_v = VELOCITY GRADIENT

$= \dfrac{D_p N_p}{D_m}$

K_t = TORQUE GRADIENT

$= \dfrac{D_p D_m N_p}{L_p + L_m}$

MOTOR

θ_m = MOTOR SHAFT POSITION

Q_m = MOTOR FLOW

L_m = MOTOR LEAKAGE

D_m = MOTOR DISPLACEMENT

J_m = MOTOR INERTIA

LOAD

J_L = LOAD INERTIA

$J = J_m + \frac{1}{n^2} J_L$

Figure 21—Hydraulic Drive System

$$\frac{\theta}{V_f} = \frac{\dfrac{K_g}{K_v R_f}}{s\left(s^2 \dfrac{L_a J}{K_t K_v} + s\dfrac{J R_a}{K_t K_v} + 1\right)\left(s\dfrac{L_f}{R_f} + 1\right)} \tag{32}$$

The quadratic factor has a natural frequency ω_n and damping factor ζ of:

$$\omega_n = \sqrt{\frac{K_t K_v}{L_a J}} \tag{33}$$

$$\zeta = \frac{R_a}{2}\sqrt{\frac{J}{K_t K_v L_a}} \tag{34}$$

5.2 Hydraulic Drive

The prime mover in a hydraulic drive could be a linear or rotary actuator for low horsepower applications or a hydraulic motor. Actuators can be connected directly to the load without gearing and have the advantage of low inertia and fast response. In applications where continuous rotation or high horsepower is required, hydraulic motors have to be used. Prime movers can be excited by either a servo valve or a variable displacement pump. The valve has the advantage of faster response over the pump but has the disadvantage of low power efficiency and of suffering degradation in performance due to contamination of the hydraulic fluid. Pumps which are preferred in the higher horsepower ranges very often require a secondary valve-piston combination to control the yoke of the pump. But this secondary loop can operate at lower pressures and much lower power level than the primary pump-motor circuit. A simplified schematic is shown in Fig. 21. To develop the transfer function relating shaft position to pump stroke, equations can be written for parts of the total pump stroke and then the parts added:

$$X_v = \frac{s}{K_v} \theta_m \tag{35}$$

$$X_a = \frac{s^2 J}{K_t} \theta_m \tag{36}$$

$$X_c = \frac{s^3 VJ}{D_m^2 K_v B} \theta_m \tag{37}$$

$$X = X_v + X_a + X_c = s \left(s^2 \frac{VJ}{D_m^2 K_v B} + s \frac{J}{K_t} + \frac{1}{K_v} \right) \theta_m \tag{38}$$

By rearranging terms, the transfer function is obtained:

$$\frac{\theta_m}{X} = \frac{K_v}{s \left(\frac{VJ}{D_m^2 B} s^2 + \frac{K_v J}{K_t} s + 1 \right)} \tag{39}$$

where the natural frequency and damping factor is:

$$\omega_n = D_m \sqrt{\frac{B}{VJ}} \tag{40}$$

$$\zeta = \frac{L_p + L_m}{2 D_m} \sqrt{\frac{BJ}{V}} \tag{41}$$

5.3 Comparison with Eddy Current Clutch Drive

Comparisons will be made between dc, hydraulic, and eddy current clutch drives at two power levels: at the simulator level or 10 hp range, and at the 85 ft antenna level or 200 hp range. To make the comparison meaningful, certain basic assumptions have to be made. Sizing of the driver will be done by using load characteristics from Table 1 and substituting these, together with driver characteristics, into the following equations to determine power requirements:

$$T = T_a + T_w + T_f \tag{42}$$

$$T_a = \text{acceleration torque (ft lbs)} = (J_L + 2N^2 J_m)\,\ddot{\theta} \tag{43}$$

T_w = wind torque (Table 1)

$$T_f = \text{friction torque (ft lbs)} = 0.1\,(T_a + T_\omega) \tag{44}$$

$$P = \text{required load power (hp)} = T\dot{\theta}/5250 \tag{45}$$

where

J_L = load torque (Table 1)

J_m = torque of driver (ft lbs sec^2)

N = gear ratio

After the driver is sized, the dynamic response will be determined by using equations 33 and 34 for dc, 40 and 41 for hydraulic, and 15 for eddy current clutch drives.

Table 3 shows comparisons between the various systems. Care has to be exercised in using numbers from this table, inasmuch as the numbers have to be interpreted correctly and should not be used indiscriminantly as an absolute measure.

Table 3 – Comparison

Characteristic	Simulator Size					Full Size	
	DC–NEMA Motor	DC Torque Motor	Hydraulic Pump-Motor	Hydraulic Valve Motor	Eddy Current Clutch	Hydraulic Pump-Motor	Eddy Current Clutch
PRIME MOVER							
Manufacturer	GE	Inland	Vickers	Vickers	Eaton	Vickers	Eaton
Part Number	504	T-18004-A	Model A	Model B	WCS 2062	MFA 120	WCS 216
Power – hp	15	11.4	9	14.2	10	200	220
Speed – rpm	300	60	12,500	10,000	1200	1800	1200
Inertia – slug ft^2	1.43	3.1	1.56×10^{-5}	4.73×10^{-5}	.155	.292	1.92
Torque to Inertia Ratio – ft lbs/sec^2	98,000	323,000	7,900	15,400	16,800	8,230,000	634,000
Weight–lbs per unit	1915	600	1.7	3.3	270	600	1900
POWER GENERATOR							
Type	Amplidyne	Amplidyne	Pump	Valve	AC Motor	Pump	AC Motor
Manufacturer	GE	GE	Vickers	Moog	Westinghouse	Vickers	
Part Number	624 F	622 F	Model A	Series 32	284 US	PVA 120	
Power – hp	20	13.5	9	4.7	10	200	350
Speed – rpm	1750	1750	12,500	N/A	1160	1200	1160
Weight – lbs	825	600	1.7	.75	290	1150	3100
SYSTEM							
Weight – lbs	4655	1200	5.1	7.4	830	2,350	10,000
Natural Frequency	61.4	36.8	200	412	5.78	122	7.1
Damping Factor	.145	.416	.0276	.038	.292	.0528	.355

For low horsepower ranges several drive types have been considered, but in the high horsepower class only two practical drives are mentioned. Dc motors, because of their high inertia, cannot be used unless special designed motors are developed with smaller rotors.

When the prime mover characteristics are considered a variation of horsepower levels is noticed. For the simulator size drives this variation is mainly caused by steps in component ratings. For example, in the dc motor drive about 12 hp are required, but the available size closest to this is a 15 hp unit. The valve-motor drive seems to require a larger unit than the pump-motor drive. This is not because a larger load is encountered but because the smaller motor would require a system pressure of over 3000 psi, which is generally undesirable. For full-size drives the eddy current clutch requires a higher horsepower rating than the hydraulic drive because of its high acceleration torque requirement due to higher inertia of the clutch.

Inertias seem to vary considerably for different drives, but so do the shaft speeds of these drives. To make a better comparison, inertias that are referred to a particular speed should be considered. Such a comparison is made graphically in Fig. 22. As can be seen from this figure, eddy current clutches have higher inertias than their dc motor counterparts up to a rating of 100 hp; above that the situation reverses. Hydraulic motors have a decided advantage in inertia over both motors and clutches.

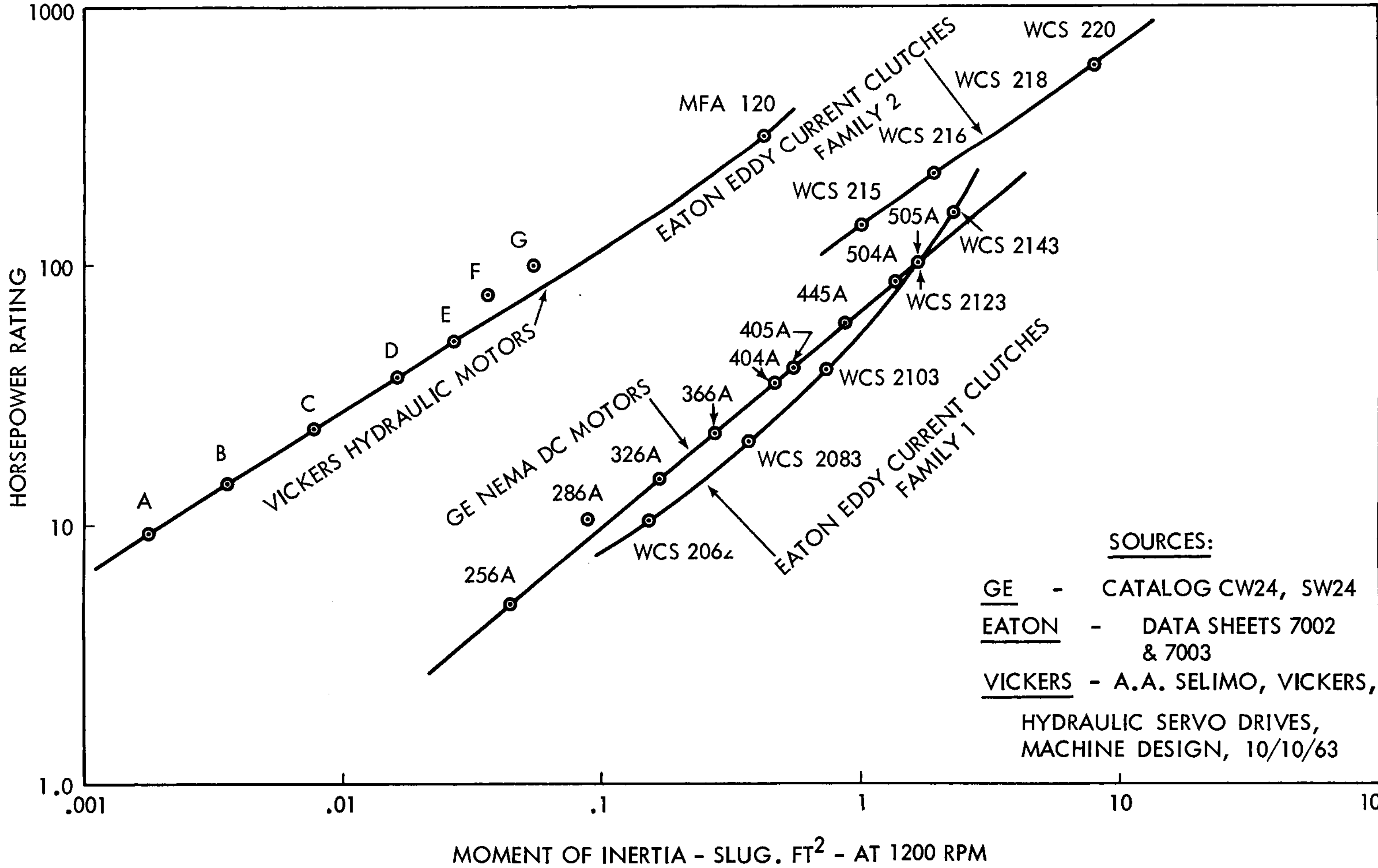

Figure 22—Comparison of Inertias

A figure of merit in the motor is the torque to inertia ratio or the torque-squared to inertia ratio. The latter is sometimes preferred because it remains constant at both ends of a gear reducer. At simulator power levels, the dc motors and in particular the dc torque motor are the preferred units, while the eddy current clutch runs second. At the high power level, though, the hydraulic motor has an advantage over the clutch.

From a weight standpoint the hydraulic motor is by far the preferred unit, but the eddy current clutch is lighter than the dc motor. These figures, however, are somewhat misleading as far as dc motors are concerned. The torque motor requires no gearing, but all other units do. Consequently a weight for the appropriate gear reducer should be considered. Also a low speed NEMA motor was chosen for the comparison. If weight is a major system design criteria, a 3500 rpm motor could be chosen in place of a 300 rpm unit, which reduces the weight from 1915 lbs to 285 lbs. The figures in the table also do not take into account that special designs could be arrived at that would demonstrate much improved characteristics. Power generators also make hydraulics more attractive than the eddy current clutch and dc motors as far as weights are concerned.

Total system weights given in the table are the sum of prime mover and power generator weights. These figures neglect weights of electronic controllers, gearing, mounting hardware, reservoirs and piping for hydraulic systems, cooling system for eddy current clutch systems, etc. All of these factors would have to be considered in arriving at a total system weight. Indications are that the hydraulic system still will be lighter than the clutch or dc motor systems.

To study the transient response, it is sufficient for a preliminary check to determine the predominant natural frequency and damping factor. For the dc and hydraulic drives this can be done simply by using equations 33, 34, 40, and 41. The clutch drive because of the type of its transfer function, does not lend itself to direct comparison. To put all systems on an equal basis, a tachometer feedback will be introduced with an arbitrarily chosen loop gain of 10. This addition modifies the original natural frequency ω_n and damping factor ζ for dc and hydraulic drives as follows:

$$\omega_n/\text{modified} = \omega\sqrt{11} \tag{46}$$

$$\zeta/\text{modified} = \frac{\zeta}{\sqrt{11}} \tag{47}$$

The transfer function of the clutch drive G_c is modified by the feedback H_c to give a new G_c':

$$G_c = \frac{K_t/JR}{s^2\left(s\frac{L}{R}+1\right)} \tag{15}$$

$$H_c = s\,Kg \tag{48}$$

$$G_c' = \frac{G_c}{1 + G_c H_c} = \frac{1/K_g}{s\left(s^2 \frac{LJ}{K_g K_t} + s \frac{RJ}{K_g K_t} + 1\right)} \tag{49}$$

where

$$\omega_n/\text{clutch} = \sqrt{\frac{K_g K_t}{LJ}} \tag{50}$$

$$\zeta/\text{clutch} = \frac{R}{2}\sqrt{\frac{J}{K_g K_t L}} \tag{51}$$

$$K_g = 10\,\frac{JR}{K_t} \tag{52}$$

Substituting values into equations 46, 47, 50, and 51, the predominant natural frequency and its damping factor is obtained and entered in Table 3. It is assumed here that the predominant natural frequency is the sole determining factor for bandwidth. Consequently this frequency is somewhat hypothetical because other time constants have been neglected which could influence bandwidth. But, if a further assumption is made that all of these other effects are present in all drive systems to approximately the same degree, then the natural frequency does represent an index of performance in the comparison of various systems.

Among the low horsepower drives the hydraulic valve-motor system has the highest natural frequency of 412 rad/sec, with the pump-motor system second with 200 rad/sec. One characteristic of hydraulic drives is that a high loss in piping is encountered. For example, if the piping length were doubled for the pump-motor system, the natural frequency would drop to 128 rad/sec. This equivalent effect is not present in dc motor or eddy current clutch drives; doubling lead length will not affect performance significantly. Also, the hydraulic drives are highly underdamped; but adjustments of the tachometer loop could easily improve this situation. Dc motor drives have a smaller bandwidth than hydraulic but exceed clutch drives by a good margin. The fact that the clutch drive has a natural frequency of only 5.78 rad/sec is not necessarily a limiting factor for system design; it just makes compensation more difficult. For the full-size drive the hydraulic system is preferred over the clutch system because of a much larger bandwidth.

So far, in comparing drive systems, use has been made of the numbers in Table 3; and the hydraulic systems seem to be superior. However, to complete the comparison, other factors have to be considered-factors that do not lend themselves readily to being put into numbers.

The first of these factors is reliability. The clutch drive has a limitation on life because of wearing mechanical parts, namely bearings and and coolant seals. Besides bearings and oil seals, the hydraulic drive has more moving parts, i.e., pistons, yokes, and other parts which tend to lower the reliability. The reliability is affected also by possible contamination of the fluid. Contamination is caused by introduction of impurities like sand, dirt, metal filings, etc. during assembly and during operation of the system due to wear of hydraulic components. Chemical changes of the fluid due to extreme temperature and pressure changes tend to add sludge and gum. A conservative estimate of mean-time-between-failure (MTBF) for a 200 hp drive is 16,500 hours for the hydraulic system and 36,500 hours for the clutch system, thus giving the latter system a better than 2:1 margin. Dc motor systems should have a MTBF similar to that of the clutch system except that brush and commutator wear has to be taken into account, thus lowering the MTBF by some amount.

Maintenance is very closely related to reliability; thus the hydraulic system requires more maintenance than the clutch drives. In the clutch drive maintenance consists mainly of greasing bearings and checking the coolant level. Hydraulic system maintenance requires regular oil changes, system cleaning, greasing of bearings, tightening of fittings, changing of filter elements, etc.

Another factor not considered in Table 3 is RFI. Hydraulic systems by nature do not generate RFI. Eddy current clutch drives, because of their construction, do not have slip rings or commutators and thus also do not generate RFI, the only exception being the fact that a relative large dc field excitation is required on the clutches. If this excitation is derived from a commutating source such as SCR's, thyratrons, or dc generators, RFI may appear. This can be prevented however by choosing the proper amplifier or by using RFI filters and good shielding practices. Dc motor drives are inherent RFI generators, but by proper design successful drive systems can be developed.

5.4 Other Clutches

Before leaving the topic of comparisons, it may be in order to mention other types of clutches and how they compare with the eddy current clutch. Other types are friction disk, crystal, loudspeaker, hysteresis, magnetic particle, and magnetic fluid clutches.

Friction disk clutches are either mechanically or electrically operated devices similar to ordinary automobile clutches. These units can transmit high torques, have a relative low durability, and are basically suited for on-off operation only. Friction disk clutches are not suited for antenna drive applications. Crystal and loudspeaker clutches, even though utilizing different principles, are on-off devices. Their low power rating puts them into the instrument servo class rather than a power drive class.

Lately a lot of interest has been shown in the application of hysteresis clutches for instrument servos and low horsepower systems. However, no information is available on developments of higher horsepower units.

Magnetic particle and fluid clutches are available with characteristics close to those of the eddy current clutch. Basically, these clutches consist of two disks separated by an airgap which is filled with magnetic powder or magnetic particles suspended in fluid. A magnetic field causes the particles to form a more or less rigid bond between the plates, depending upon the excitation level. This bond is capable of transmitting torque independent of the speed of the clutch. Magnetic particle and fluid clutches up to about 100 hp ratings are available commercially. Similar to the eddy current clutch, these clutches are subjected to high slip power causing heat dissipation problems. Excessive heat could chemically affect the magnetic particles to cause a change in their characteristics. Magnetic particles also cause sealing and wear problems and pose a difficult design requirement, which necessitates that the particles be distributed evenly in the airgap under all operating and non-operating conditions.

6. CONCLUSION

On the basis of comparisons between hydraulic, dc, and eddy current clutch drives, it can be concluded that the clutch drive has one major advantage: That is in reliability and consequently decreased maintenance requirements. Disadvantages are relatively high inertia and therefore a poor torque to inertia ratio, predominant field time constant which limits bandwidth, non-linear operation, and heat dissipation problems which cause poor efficiency. But despite these disadvantages it is possible to design and build a satisfactory control system that assures required stability and tracking accuracy.

Historically, the eddy current clutch has been used for many years in automatic machinery, but very few applications are known to antenna systems. One of NASA's antennas on Wallops Island had an eddy current clutch drive. This antenna was designed and built by General Bronze, a company which has since discontinued the manufacture of antennas.

The drive system of this particular antenna has a history of burned-out clutches due to excessive heat dissipation and poor control ability. However the general opinion is that this situation was not caused by inherent problems with the clutch but rather by choosing an underrated unit because of lack of information on and experience with clutches. Eddy current clutch drives were proposed for the 250 ft antenna of JPL and the 600 ft Sugar Grove antenna of the Navy. The latter antenna system was to utilize clutch drives but the whole project was cancelled before completion, and consequently the drive system could not be tested and evaluated.

To prove conclusively the advantages or disadvantages of the eddy current clutch drive system over the hydraulic drive, it is necessary to build a full-size clutch drive. Only then, after several months of operations under realistic conditions, can a firm opinion be formed. While certain characteristics of the hydraulic drive are superior to those of the eddy current clutch as has been pointed out here, either drive appears capable of meeting all dynamic performance specifications so that these differences are of secondary importance in the application under consideration. In view of the down-time experience with the present hydraulic drives the reliability factor becomes the most important characteristic when making a comparison. If the clutch system should prove itself more reliable by a reasonable factor, and should no unusual problems develop such as excessive heating, poor control, etc., it will be well worthwhile to choose eddy current clutches for future applications and even to consider modification of present antennas. Reliability of the drive system is very important since it is expensive to have down-time on a multimillion dollar antenna system because of a hydraulic leak or a clogged servo valve.

REFERENCES

1. W. O. Osbon, R. F. Leepa, R. F. Smith, "Electric Drive System Study for 85 ft Data Acquisition Antennas," Westinghouse Electric Corp. March 1963.

2. A. M. Flidlider, "Transient Responses in the Magnetic Circuits of Electromagnetic Clutches," Automatika i Telemekhanika, Vol. 20, No. 1, pp. 31-44.

3. P. N. Kopai-Gora, "Concerning Some Properties of Ferromagnetic Clutches," Automatika i Telemekhanika, Vol. 19, No. 4, pp. 366-375.

4. J. G. Truxal, "Control Engineer's Handbook," McGraw-Hill Book Co., 1958.

5. H. Chestnut and R. W. Mayer, "Servomechanisms and Regulating System Design," Volume 2, John Wiley and Sons, 1955.